

**T.C.  
İNÖNÜ UNIVERSITY  
INSTITUTE OF SCIENCES**

**NUCLEIC ACID BASED LATERAL FLOW TEST (LFT) FOR COVID-19  
DIAGNOSIS**

**MASTER THESIS**

**Enes GÜLTEKİN**

**Department of Molecular Biology**

**Thesis Advisor: Asst. Prof. Dr. Dilek ÇAM**

**JULY 2021**

**T.C  
İNÖNÜ UNIVERSITY  
INSTITUTE OF SCIENCES**

**NUCLEIC ACID BASED LATERAL FLOW TEST (LFT) FOR COVID-19  
DIAGNOSIS**

**MASTER THESIS  
Enes GÜLTEKİN  
36193623004**

**Department of Molecular Biology**

**Thesis Advisor: Asst. Prof. Dr. Dilek ÇAM**

**JULY 2021**



## **ACKNOWLEDGEMENTS**

I would like to thank my advisor, who has always given me the opportunity to improve myself in the academic world, from the beginning to the end of this process. Instructor I would like to express my sincere and deepest gratitude to its member Dilek ÇAM for her encouragement, valuable advice, guidance and insights.

I would like to express my gratitude and respect to my extended family for their unwavering support.

I would like to thank İnönü University Scientific Research Project (BAP) unit for their moral and material support to the project whose project code was TYL-2021-2413 and project ID 2413 during the application phase of the thesis.

## **WORD OF HONOR**

I declare that, this “Nucleic Acid Based Lateral Flow Test (LFT) For COVID-19 Diagnosis” titled study that I submit as a master thesis is written on my own without consulting an assist that contrary to academic ethics and tradition, and all literature, both in text and reference, I utilize is consisted that are displayed in reference appropriate to the method and I confirm this with my honor.

Enes GÜLTEKİN



## TABLE OF CONTENTS

<b>ACKNOWLEDGEMENTS.....</b>	<b>i</b>
<b>WORD OF HONOR.....</b>	<b>ii</b>
<b>TABLE OF CONTENTS.....</b>	<b>iii</b>
<b>LIST OF TABLES.....</b>	<b>vi</b>
<b>LIST OF FIGURES.....</b>	<b>vii</b>
<b>LIST OF ABBREVIATIONS.....</b>	<b>viii</b>
<b>ÖZET.....</b>	<b>ix</b>
<b>ABSTRACT.....</b>	<b>x</b>
<b>1. INTRODUCTION.....</b>	<b>1</b>
1.1 Coronavirus.....	1
1.1.2 Middle East Respiratory Syndrome (MERS).....	3
1.1.3 Severe Acute Respiratory Syndrome-2 (SARS-2).....	4
1.2 Structural Protein of SARS-CoV-2.....	5
1.2.1 Spike (S) Protein.....	5
1.2.2 Nucleocapsid (N) Protein.....	6
1.2.3 Membrane (M) Protein.....	8
1.2.4 Envelope (E) Protein.....	8
1.3 SARS-CoV-2 Detection Methods.....	8
1.3.1 Molecular diagnostic tests.....	8
1.3.1.1 Polimerase Chain Reaction (PCR) based diagnosis.....	9
1.3.2 Serological diagnostic tests.....	10
1.3.2.1 Antigen detecting diagnostic tests.....	10
1.4 Lateral Flow Test (LFT) Based Diagnosis.....	12
1.5 Aim of the Study.....	14
<b>2. MATERIALS AND METHODS.....</b>	<b>15</b>
2.1 Materials.....	15
2.1.1 Chemicals and reagents.....	15
2.1.2 Buffers and solutions.....	16
2.1.3 Test strip components.....	17
2.1.4 Synthetic oligonucleotides.....	17
2.2 Methods.....	19
2.2.1 Gold nanoparticle synthesis.....	19
2.2.1.1 Conjugation of AuNPs with thiolated oligo probes.....	19
2.2.2 Preparation of test components.....	20

2.2.3 Assembly of lateral flow test strip.....	20
2.2.4 PCR conditions for N protein sequence.....	21
2.2.5 Agarose gel electrophoresis of PCR products.....	22
2.2.6 Assay procedure for the synthetic target.....	22
2.2.7 Assay procedure for PCR products.....	22
2.2.8 Hybridization models used in LFT.....	23
<b>3. RESULTS AND DISCUSSION.....</b>	<b>24</b>
3.1 Synthesis of Gold Nanoparticles.....	24
3.2 Functionalization of Conjugate Probes.....	25
3.3 N Gene PCR.....	27
3.4 The Working Principle of LFT.....	28
3.5 Temperature Optimization Experiments.....	28
3.6 Buffer Optimization Experiments.....	30
3.7 LFT for PCR Product.....	32
3.8 Result of Model 2.....	33
3.9 Limit of Detection.....	34
<b>4. CONCLUSION.....</b>	<b>38</b>
<b>REFERENCES.....</b>	<b>39</b>
<b>CURRICULUM VITAE.....</b>	<b>44</b>

## LIST OF TABLES

<b>Table 2. 1 :</b> Buffer tables.....	16
<b>Table 2. 2 :</b> Sequences and modifications of synthetic probes for N gene detection.....	18
<b>Table 2. 3 :</b> PCR Conditions for 72bp of N gene.....	21
<b>Table 2. 4 :</b> Optimized PCR conditions for 72 bp amplicon.....	21





## LIST OF FIGUR

<b>Figure 1. 1</b> : Sequence characteristics of COVID-19 N protein.....	7
<b>Figure 1. 2</b> : Schematic representation of the lateral flow test.....	13
<b>Figure 2. 1</b> : Plot of detection of target nucleic acids by sandwich hybridization.....	23
<b>Figure 3. 1</b> : UV-Vis Spectrum of synthesized AuNPs (A) and 4X concentrated AuNPs (B) .....	24
<b>Figure 3. 2</b> : AuNP-Probe conjugations for model 1 and model 2.....	25
<b>Figure 3. 3</b> : Absorption spectrum of 4 $\mu$ M(A) and 8 $\mu$ M(B) oligo conjugate model 1.....	26
<b>Figure 3. 4</b> : Absorption spectrum of 4 $\mu$ M(A) and 8 $\mu$ M(B) oligo conjugate model 2.....	26
<b>Figure 3. 5</b> : Agarose gel image of PCR product.....	27
<b>Figure 3. 6</b> : Temperature optimization for LFTs using Whatman 2 membrane.....	28
<b>Figure 3. 7</b> : Temperature optimization for LFTs using Whatman 1 membrane.....	29
<b>Figure 3. 8</b> : Buffer optimization for LFTs using 4 $\mu$ M model 1.....	30
<b>Figure 3. 9</b> : Buffer optimization for LFTs using 8 $\mu$ M model 1.....	31
<b>Figure 3. 10</b> : N3 PCR product (6 $\mu$ L) LFT using Whatman 2 membrane with model 1.....	32
<b>Figure 3. 11</b> : Model 2 LFT result.....	33
<b>Figure 3. 12</b> : Limit of detection experiments with Whatman 2-membrane Model 1.....	34
<b>Figure 3. 13</b> : Limit of detection experiments with Whatman 2-membrane Model 2.....	35
<b>Figure 3. 14</b> : Limit of detection experiments with Whatman 1-membrane Model 1.....	36
<b>Figure 3. 15</b> : Limit of detection experiments with Whatman 1 membrane Model 2.....	37

## LIST OF ABBREVIATIONS

<b>AuNP</b>	: Gold Nanoparticle
<b>DNA</b>	: Deoxyribonucleic Acid
<b>PBS</b>	: Phosphate Buffered Saline
<b>RT-PCR</b>	: Real Time Polymerase Chain Reaction
<b>RNA</b>	: Ribonucleic Acid
<b>SSC</b>	: Saline-Sodium Citrate
<b>TCEP</b>	: Tris(2-Carboxyethyl)phosphine
<b>RB</b>	: Running Buffer
<b>N</b>	: Nucleocapsid
<b>NCM</b>	: Nitrocellulose membrane
<b>LFT</b>	: Lateral flow test
<b>BSA</b>	: Bovine serum albumin
<b>RT</b>	: Room temperature

## ÖZET

Yüksek Lisans Tezi

NÜKLEİK ASİT TEMELLİ YANAL AKIŞ TESTİ (LFT) İLE COVID-19 TESPİTİ

Enes GÜLTEKİN

İnönü Üniversitesi

Fen Bilimleri Enstitüsü

Moleküler Biyoloji Anabilim Dalı

44+X sayfa

2021

Danışman: Dr. Öğr. Üyesi Dilek ÇAM

Dünya Sağlık Örgütü (DSÖ) tarafından resmi adı SARS-CoV-2 (Şiddetli Akut Solunum Sendromu-Koronavirus-2) olarak belirlenen yeni koronavirüs, ilk kez 2019 yılı Aralık ayı sonlarında Çin'in Wuhan şehrindeki deniz ürünleri pazarında ortaya çıktığı düşünülmektedir. Virüs oldukça bulaşıcı ve özellikle ileri yaş gruplarında ölümcül olmaktadır. Viral teşhis için birçok çalışma geliştirilmeye devam etmektedir. En yaygın ve güvenilir olanı DSÖ tarafından önerilen RT PCR (Real Time Polymerase Chain Reaction) olup özellikle N geni bölgelerine yöneliktir. Bu bölge en korunaklı ve spesifik bölge olduğu için moleküler teşhiste önemli olmuştur. Bununla birlikte hızlı testler laboratuvar yüklerinin hafifletilmesinde, antikor gelişimini kontrol etmede önemli yere sahiptir. Hızlı testler arasında ise yatay akışlı testler en yaygın ve pratik kullanımı olanıdır. Uzun vadede viral bulaşıklık ihtimali hep olacaktır ve pratik kullanımlı teşhis testlerine ihtiyaç devam edecektir. Bu amaçla çalışmamızda SARS-CoV-2'ye özgü N geni bölgelerinin yatay akışlı hızlı test platformu ile teşhisi hedeflenmiştir.

Yatay akışlı test platformu Altın nanoparçacıklara (AuNP) dayalı sandviç modeli ile hibridizasyon temeline dayalı olarak tasarlanmıştır. Tasarlanan LFT platformu N geninin korunmuş bölgelerine özgü dizayn edilmiştir. N genine tamamlayıcı olan DNA oligonükleotitleri ile AuNP konjuge edilmiştir.

Bu konjugasyon ürününe hibridizasyon oluşturacak diziler nitroselüloz membran üzerine test ve kontrol çizgisi olarak çizilmiştir. Hedef sekansı içeren örnek, numune pedine uygulandığında kapiller akım prensibine dayanarak hedef sekans test ve kontrol çizgisinde bulunan diziler ile hibridizasyon yapar. AuNP'den kaynaklı bir kırmızı renk oluşumu çıplak gözle görülebilir. Araştırma bulgularına göre, tasarlanan LFT, SARS-CoV-2 N geni bölgelerini spesifik olarak tanıyış ve moleküler teşhise alternatif olabileceği ortaya konmuştur.

**Anahtar kelimeler:** LFT, SARS-CoV-2, Teşhis, COVID-19

## ABSTRACT

Master Thesis

NUCLEIC ACID BASED LATERAL FLOW TEST (LFT) FOR COVID-19 DIAGNOSIS

Enes GÜLTEKİN

Inonu University

Graduate School of Nature and Applied Sciences

Department of Molecular Biology and Genetic

44+X page

2021

Thesis advisor: Asst. Prof. Dr. Dilek ÇAM

The new coronavirus, official name was determined by the WHO as SARS-CoV-2, is thought to have first appeared in the seafood market in Wuhan, China, in late December 2019. The virus is highly contagious and fatal, especially older age groups. Many studies continue to be developed for viral diagnosis. The most common and reliable one is the RT PCR recommended by WHO, and it is especially aimed at the N gene regions. This region has been important in molecular diagnosis as it is the most conserved and specific region. However, rapid tests have an important place in relieving laboratory and controlling antibody development. Among rapid tests, LFTs are the most common and practical. In long time, there will always be the possibility of viral contamination and the need for practical diagnostic tests will continue. For this purpose, our study aimed to identify the N gene regions specific to SARS-CoV-2 with a LFT platform. The LFT platform is designed on the basis of hybridization with sandwich model based on Gold nanoparticles (AuNP). The designed LFT platform was designed specifically for the conserved regions of the N gene. AuNP was conjugated with DNA oligonucleotides complementary to N gene. Sequences that will hybridize to this conjugation product were drawn on the nitrocellulose membrane as test lines. The sample containing the target sequence hybridizes with the sequences in the test and control lines based on the capillary flow principle when applied to the sample pad. A red color formation from AuNP can be seen with the naked eye. According to the research findings, the designed LFT specifically recognized the SARS-CoV-2 N gene regions and it was revealed that it could be an alternative to molecular diagnosis.

**Keywords:** LFT, SARS-CoV-2, Diagnosis, COVID-19

**To My Family**



# 1. INTRODUCTION

## 1.1 Coronavirus

On December 31, 2019, the World Health Organization (WHO) China Office reported cases of pneumonia of unknown etiology in Wuhan, China's Hubei province. On January, 2020, this virus was reported to be a new coronavirus that had not been detected in humans before and was identified as 2019-nCoV. However, the name of the 2019-nCoV disease was later accepted as COVID-19, and the virus was named SARS-CoV-2 due to its close similarity to SARS CoV (Yu, J., et al., 2020). The coronavirus disease 2019 (COVID-19) pandemic caused by the new severe acute respiratory syndrome coronavirus 2 (SARS-CoV-2) caused a significant increase in hospitalizations as a result of pneumonia manifested by sudden and multi-organ diseases worldwide (Harapan et al., 2020). Coronaviruses affect humans, livestock, birds, mice, bats, wild animals and cause gastrointestinal, respiratory, and central nervous system disorders (Xu, J., et al., 2020). In humans, coronavirus infections first affect the upper respiratory tract, then the gastrointestinal system and many organ systems. Multiple organ failure is seen due to the extreme progress of the disease, and this situation causes death (Su, S., et al., 2016).

Coronaviruses are zoonotic and they are members of a large family of viruses that can infect humans (Su, S., et al., 2016). Coronaviruses typically have a narrow host range and can cause serious illness in many animals; infectious bronchitis virus, feline infectious peritonitis virus and infectious gastroenteritis virus are the most important pathogenic viruses among coronaviruses. These viruses are also transmitted from animals to humans and cause serious diseases (Kuru, T. T., Asrat, D., 2004).

Coronaviruses are studied in different groups. Differences in the genomic structure of the virus and its antigenic interactions with the host cell are important in the differentiation of these groups (Yücel, B., Görmez, A. A., 2019).

Although there is no complete information about the coronavirus diversity on our planet, there are 7 types of coronaviruses known to infect humans. The severity of respiratory symptoms varies depending on the type of virus.

Four of these viruses (HCoV-229E, HCoV-OC43, HCoV-NL63 and HKU1-CoV) are responsible for almost half of common colds in humans (Ludwig, S., Zarbock, A., 2020). Researchers initially thought that coronaviruses cause only mild cold and flu-like symptoms in humans. However, in the last 20 years, 2 strains have triggered alarming disease outbreaks. The virus (SARS-CoV) that causes Severe Acute Respiratory Syndrome (SARS), which also appeared in China in 2002, killed more than 770 people worldwide, while another one, Middle East Respiratory Syndrome (MERS-CoV), emerged in the Middle East (Saudi Arabia and Jordan) in 2012 and killed more than 800 people. While SARS disappeared within a year, MERS still continues. As a result of detailed research, it has been revealed that SARS-CoV is transmitted from musk cats and MERS-CoV from dromedary camels to humans. There are many coronavirus that have not yet been transmitted to humans but are detected in animals (Li, F., 2016).

Coronaviruses are viruses having an envelope, single RNA strand, and positive polarity. Since they have positive polarity, they do not contain RNA-dependent RNA polymerase, but they have a gene encoding this enzyme in their genome. There are rod-like extensions on their surfaces and these viruses are named as Coronavirus (crowned virus), starting from the Latin equivalent of "corona", that is, "crown" (Heald-Sargent, T., Gallagher, T., 2012).

At the end of 2002, an unusual life-threatening respiratory tract epidemic of unknown etiology began in Guangdong Province, China (Drosten, C., et al., 2003). In the last two decades, it has been two crucial coronavirus epidemics, SARS-CoV (2002) and MERS (2012) (Cui, J., et al., 2019). SARS-CoV-2 and other coronaviruses, SARS-CoV and MERS-CoV are quite similar genetic and at the protein production level (Hatmal, M. M., et al., 2020).

### **1.1.1 Severe Acute Respiratory Syndrome (SARS)**

Sars Corona Virus (SARS CoV) is a coronavirus that was first seen in China in February 2003 and causes severe acute respiratory syndrome (Kuru, T. T., Asrat, D., 2004). SARS-CoV generally causes disease in animals. It is estimated that the SARS-CoV seen in

humans most likely originated from bats and coincidentally infected humans. As most common cold viruses, SARS-CoV is relatively resistant and highly contagious RNA virus. It is spread from person to person by respiration, as a result of contact with contaminated fomites, body fluids or feces.

The fact that approximately 20% of the infections are in healthcare workers indicates the high infectivity of the virus. Close contact is especially important in contamination (Yücel, B., Görmez, A. A., 2019). SARS-CoV binds to CEACAM1 receptors, known as adhesion molecules, found on the cell surface of humans and animals in various tissues such as epithelial cells, leukocytes and tumor cells. After this interaction, the genome of the virus enters the host cell (Yang, Y., et al., 2020). SARS-CoV reaches the respiratory tract through the droplet inhalation and occupies the epithelial cells of the trachea, bronchi, bronchioles and alveoli (Guo, Y., et al., 2008). SARS-CoV typically causes a wide range of illnesses, including symptoms such as high fever, weakness, chills, and fatigue (Cameron MJ, et al., 2008). In general, a typical respiratory phase including non-productive cough and shortness of breath is initiated 2 to 7 days after the onset of SARS. In two-thirds of infected patients, the disease worsens to atypical pneumonia with shortness of breath and poor alveolar oxygen exchange (Perlman S, Dandekar AA., 2005). According to WHO reports, 8096 people were infected with the SARS-CoV and 774 (9.6%) people died in 11 countries (Luk, H. K., et al., 2019).

The size of the genome of SARS CoV can range from 29 kb to 30.2 kb. This genome is packaged in a helical capsid formed by the nucleocapsid protein (N) and surrounded by an envelope. There are three structural proteins (M, E, S) related with viral envelope. Although membrane protein (M) and envelope protein (E) provide a complete mature virus formation, the pointed protein (S) selects the host cells and determines the cells which the virus will enter (Li, F., 2016).

Two-thirds of the 5' region of the SARS CoV genome encodes non-structural proteins, while one-third of the 3' region encodes structural proteins (Luk, H. K., et al., 2019).

### **1.1.2 Middle East Respiratory Syndrome (MERS)**

In 2012, a new betacoronavirus emerged in the Arabian Peninsula which is called as Middle East respiratory syndrome coronavirus, MERS-CoV, and is associated with



severe respiratory disease in humans (De Wit, E., et al., 2013). Common symptoms of MERS-CoV include tremor, chills with chills, migraine, cough, sore throat, difficulty breathing, muscular rheumatism, chest pain, kidney failure, pneumonia, dizziness, nausea and vomiting, dysentery and stomach pain. The first case of Middle East Respiratory Syndrome was detected in a patient with acute pneumonia and kidney failure in Jeddah, Saudi Arabia (Zaki, A. M., et al., 2012).

The source of the virus is usually animals with the inclusion of bats, camels and chimpanzees.

It has been reported to be transmitted from animals to humans and from person to person (Al-Hazmi, A., 2016) via droplet infection or touching to contaminated surfaces (Chu, D. K., et al., 2014). The MERS-CoV incubation period time ranges from 2 to 14 days (Zaki, A. M., 2012).

### **1.1.3 Severe Acute Respiratory Syndrome-2 (SARS-2)**

In December 2019, WHO reported on an as-yet unknown outbreak of pneumonia in Wuhan, Hubei Province, China. On January 30, 2020, WHO declared severe acute respiratory syndrome-2 (SARS-CoV-2) as an epidemic. On February 11, 2020, WHO named the current coronavirus outbreak as Coronavirus Disease 2019 (COVID-19) and finally as SARS-CoV-2 (Wang, M. Y., et al., 2020). It was reported that SARS-CoV-2 displayed the typical features of the coronavirus family which is betacoronavirus family (Lai, C. C., et al., 2020). Early in the pneumonia outbreak in Wuhan, scientists sequenced the full genome from five patients infected with SARS-CoV-2. It was revealed that SARS-CoV-2 has 79.5% similarity to SARS-CoV. SARS-CoV-2 is considered to be different from SARS-CoV and is a novel betacoronavirus that infects humans (Zhou, P., et al., 2020).

The natural reservoir of the SARS-CoV-2 is thought to be bats (Zhang, C., et al., 2020). A betacoronavirus strain isolated from pangolins, although its natural reservoir was bats, showed close to 99% similarity to the strain isolated from a patient infected with SARS-CoV-2 (Liu, Y., et al., 2020).

Another study revealed that the coronavirus isolated from SARS-CoV-2 and a pangolin in Malaysia has high genetic similarity. The gene similarity between these two viruses in terms of E, M, N and S genes is 100%, 98.6, 97.8 and 90.7, respectively. These

similarity rates increased the likelihood of pangolines being intermediate hosts (Xiao, K., et al., 2020).

SARS-CoV-2 provides transmission through droplets (Wang, M. Y., et al., 2020). Four stages of COVID-19 disease caused by SARS-CoV-2 have been identified. The first stage is characterized by upper respiratory tract infection.

The second is the onset of dyspnoea and pneumonia, the third is worsening clinical scenario dominated by a cytokine storm resulted with hyper inflammatory state, and fourth is death or recovery (Stasi, C., et al.,2020).

The most common clinical symptoms of COVID-19 disease are dry cough, fever, and shortness of breath. Some patients may also experience other symptoms such as sore throat, headache, myalgia, fatigue, and diarrhea (Chen, N., et al., 2020).

## **1.2 Structural Protein of SARS-CoV-2**

SARS-CoV-2 is an enveloped, non-compartmentalized, positively sensitive RNA virus, approximately 65-125 nm in diameter and approximately 30 kb in size (Araf, Y., et al., 2020). SARS-CoV-2 contains 4 structural and 16 non-structural proteins (Arya, R., et al., 2021). SARS-CoV-2 forms four major structural proteins including spike (S) glycoprotein, envelope (E) glycoprotein, membrane (M) glycoprotein and nucleocapsid (N) protein, and several accessory proteins (Jiang, S., Hillyer, C., 2020).

### **1.2.1 Spike (S) Protein**

The S protein of SARS-CoV-2 is approximately 77% similar to the S protein of SARS-CoV (Arya, R., et al., 2021). S glycoprotein is a transmembrane protein found on the outer surface of the virus. It forms homotrimers protruding from the viral surface and facilitates the attachment of the virus particle to the host cells with the help of angiotensin converting enzyme 2 (ACE2) receptors located in the cells of the lower respiratory tract. The S protein interacts with a serine protease, TMPRSS2, to enter the cell (Hoffmann, M., et al., 2020). A furin-like protease in the host cell splits this S glycoprotein into two subunits. These units are an N-terminal S1 subunit and a membrane-bound C-terminal S2 domain (Astuti, I., 2020). The S1 subunit comprise a receptor binding domain (RBD) that clearly recognizes ACE2 as its receptor, and the S2 subunit ease virus fusion in transmit of host cells (Fehr, A. R., et al.,2015). The S1 subunit has two well-defined structural domains within it, the receptor binding domain (RBD) and the N-terminal galectin-like

domain (S-NTD). The RBD structure has a five-helix antiparallel  $\beta$ -layer ( $\beta$ 1-  $\beta$ 2-  $\beta$ 3-  $\beta$ 4-  $\beta$ 5) core surrounded by a short helix on either side. A ring protrudes from the main nucleus, forming a cradle-like structure for receptor binding. RBD is subject to the condition that temporarily obscures or reveals determinants of receptor binding. Down-validation refers to the inaccessible receptor, while up-validation refers to the receptor that is likely to be unstable naturally.

This conformational variability is thought to be conserved among the Coronaviridae family. The S2 subunit contains four conserved structural regions. These structural regions; It is a fusion peptide (FP), two heptad repeats (HR1, HR2) and a transmembrane region (Arya, R., et al., 2021).

### **1.2.2 Nucleocapsid (N) Protein**

The N protein is one of the structural proteins found in SARS-CoV-2 genome which is the 419 amino acid long. It consists of 3 distinct regions, the N-terminal domain (NTD)/RNA binding domain, a serine/arginine-rich (SR-rich) binding domain (LKR), and a C-terminal domain (CTD). NTD binds to the 3'-end of viral RNA and is quite different. The charged serine and arginine-rich LKR region can interact directly with RNA and play a role in cell signaling. The N-NTD, N-CTD and SR-rich domain were found to be associated with the genomic RNA of the virus through electrostatic interactions by positively charged amino acid residues and modulate relaxation by phosphorylation to the specific amino acid after entry into the cell (Rahman, M. S., et al., 2021). The N protein is the only protein that binds to the RNA genome. It has been suggested that optimal RNA binding is related to these two domains. It also plays a role in viral assembly and budding, ensuring complete virion formation. It functions at viral replication unknownly and localizes to viral replication-transcription complexes (RTC).

The N protein not only packages the viral RNA to form the helix nucleocapsid included in the budding particle but also performs additional roles during viral infection. It has been shown to function as RNA chaperone and facilitate viral RNA synthesis (Parashar ve ark., 2020). High amounts of N protein, highly immunogenic, are produced during infection. As it is immunogenic it is one of the strong targets in vaccine studies (Padron-Regalado, E., 2020).

According to the Virus Variation Resource in National Center for Biotechnology Information databank (Hatcher, E.L., et al., 2017), COVID-19 N protein coding regions are conserved according to genome datasets. In global genomic NCBI 103 epidemiology, only a few variations in the N protein (Foshan / 20SF207 / 2020 virus strain S194L, Wuhan / IVDC-HB-envF13-21 / 2020 virus strain K249I, and Guangzhou / 20SF206 / 2020 virus strain P344S) have been found. The comprehensive domain structure of the N protein of 4 coronaviruses (SARS-CoV-2, SARS-CoV, MERS-CoV, and HCoV-OC43) is shown in Figure 1.1 (Saikatendu, K.S., et al., 2007).

Although the N-terminal domain of the COVID-19 N protein is similar to other coronaviruses, its surface electrostatic potential properties are different. N region of COVID-19 has been determined as target sequence because of COVID-19 specificity. For this purpose, WHO has proposed several primer sets for molecular diagnostics for the COVID-19 N gene.

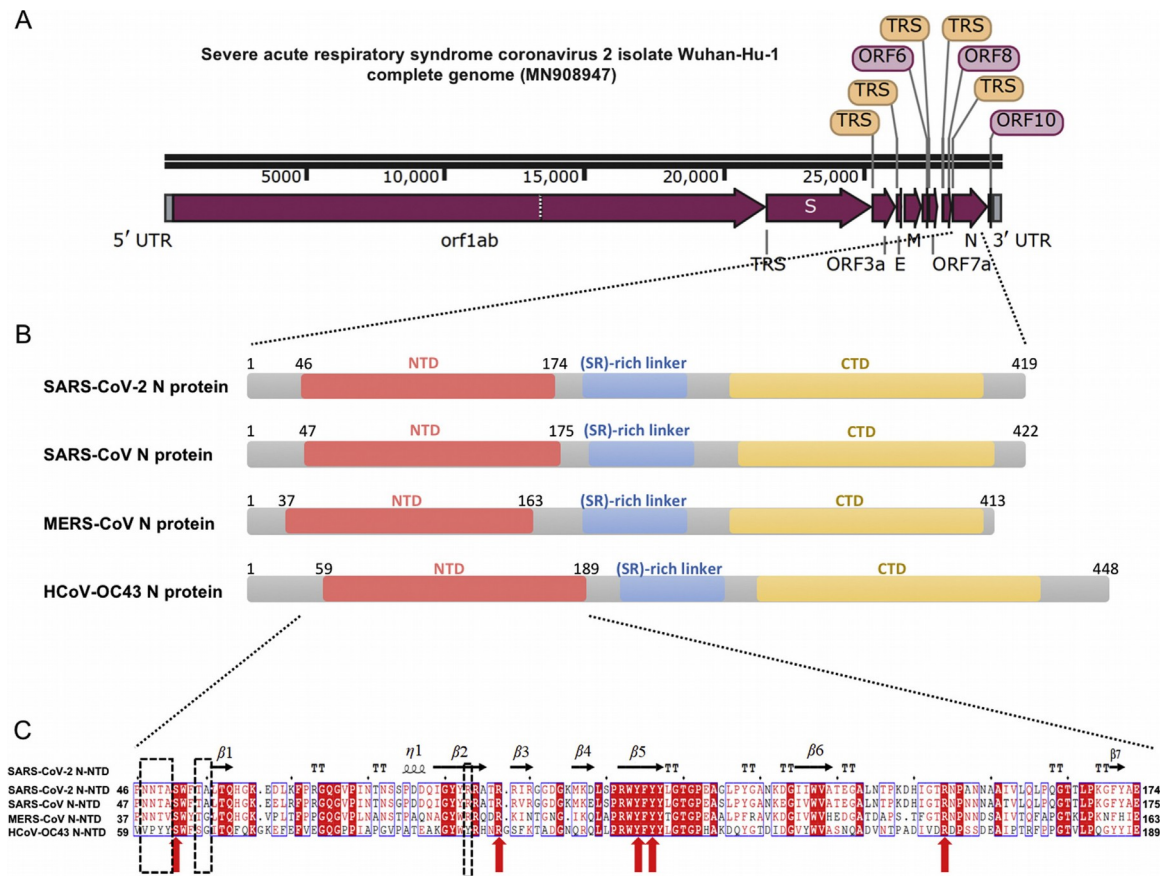


**Figure 1.1** : Sequence characteristics of COVID-19 N protein.(A) Complete genomic characteristics of Wuhan-Hu-1 COVID-19 isolate (Genebank: MN908947). UTR: untranslated region; orf / ORF: open reading frame; TRS: transcriptional regulatory sequences; S: spike glycoprotein coding region; E: envelope protein coding region; M: membrane protein coding region; N: nucleocapsid protein coding region. Figure shown by SnapGene Viewer. (B) Domain structure of the coronavirus N protein. NTD: N-terminal RNA binding domain; CTD: C-terminal dimerization domain. (C) Multiple sequence sequencing of COVID-19 N-NTD and SARS-CoV N-NTD (UniProtKB: P59595), MERS-CoV N-NTD (UniProtKB: R9UM87), HCoV-OC43 N-NTD (UniProtKB: P33469). Red arrows indicate conserved portions for ribonucleotide binding sites, dashed boxes indicate variable-shaped portions in structural comparisons (Saikatendu, K.S., et al., 2007).

### 1.2.3 Membrane (M) Protein

The M protein is the most abundant structural protein in SARS-CoV-2 and is a type III transmembrane glycoprotein. Its length is 222 amino acids. The M protein has three main domains: N-terminal ecto domain, followed by three transmembrane helix and C-terminal endo-domain. The M protein interacts with itself and other structural proteins. These interactions induce membrane bending and serve as a checkpoint for the formation of new virions (Ujike, M., Taguchi, F.,2015). M proteins are glycosylated in the Golgi

apparatus (Graham, R. L., Baric, R. S., 2010). The modification that occurs in the M protein is necessary for the virion to fuse into the cell and make the protein antigenic. The M protein plays an important role in the regeneration of virions in the cell (De Haan, C. A., et al., 2003).

#### **1.2.4 Envelope (E) Protein**

The E protein is the smallest structural protein of SARS-CoV-2 and is 75 amino acids long. It is a transmembrane structural protein. It contains 3 different domains: N-terminal hydrophilic ecto-domain, hydrophobic transmembrane domain and a long hydrophilic C-terminal endo-domain (Hong, M., et al., 2020). E proteins function in the assembly and morphogenesis of virions inside the cell (Ruch, T. R., Machamer, C. E., 2012).

### **1.3 SARS-CoV-2 Detection Methods**

#### **1.3.1 Molecular diagnostic tests**

The main molecular methods used are PCR and sequencing techniques. In light of the data obtained by SARS-CoV-2 full genome analysis, specific viral gene regions that should be used from PCR protocols have been identified. It is proposed by the WHO to investigate mainly the E gene, N gene, and RNA-dependent RNA polymerase (RdRp) enzyme gene PCR, which encodes the viral envelope protein. The method and reagents used in the detection of viral RNA, as well as the type, quality and time of sampling according to the stage of the disease, are critically important for the clinical sample to be tested.

Swab samples taken from the upper respiratory tract (nasopharynx and/or oropharynx) are widely used. Lower respiratory tract specimens such as bronchial alveolar lavage (BAL) and sputum may also be used in patients who are eligible for specimen collection.

It has been observed that the samples taken from the nasopharynx give two times better results than the samples taken from the oropharynx (Tekol, S. D., 2020). It is recommended to study the samples taken from the nasopharynx and oropharynx by combining them in a common tube. Test sensitivity has been shown to increase by testing the upper and lower respiratory tracts together (Wang, W., et al., 2020). Apart from

respiratory tract samples, SARS-CoV-2 RNA has also been isolated from stool, urine and blood samples. Due to the low sensitivity, large-scale studies are needed to determine the diagnostic value of isolation in these samples and to understand viral shedding. Such as low viral load, incorrect sampling, early or late stage sampling, antiviral drug use, inappropriate transport conditions, presence of PCR inhibitors and viral genetic mutation. False negative results are seen for reasons (Corman, V. M., et al., 2020).

### **1.3.1.1 Polymerase Chain Reaction (PCR) based diagnosis**

The genomic structure of SARS-CoV-2 plays a vital role in the design of appropriate diagnostic tests. According to the WHO, real time polymerase chain reaction (RT-PCR) amplification of 3 regions of the viral genome is required to confirm the COVID-19 disease caused by SARS-CoV-2 to test clinical samples. The most used regions for detection in clinical tests are the structural Envelope (E) region and the non-structural RNA dependent RNA polymerase (RdRp), N region RT PCR sequence (GGG GAA CTT CTC CTG CTA GAA TCA GAC ATT TTG CTC TCA AGC TGG GGG AAC TTC TCC TGC TAG AAT GGC TGG CAA TGG CGG TGA TGC TGC TCT TGC TTT GCT GCT GCT TGA CAG ATT GAA CCA GCT TGA GAG CAA AAT GTC TG). The RT-PCR protocol designed for SARS-CoV-2 involves the extraction of RNA from two regions of the viral genome and identifies these two regions within a few hours. However, cost-effective, fast and simple detection strategies are needed. A protocol has been optimized RdRp genes. This detection protocol, the mean Ct value of 4.38 for the E region and 3.85 for the RdRp region showed 100% agreement with the standard protocol. It has been found to be a sensitive and reliable method by eliminating the RNA extraction step in the direct PCR technique and eliminating the cost and time requirement of the test.

This allows the test to be used in research and facilitates screening and diagnosis in regions with less economic resources to diagnose COVID-19 (El-Kafrawy, S. A., et al., 2021).

### **1.3.2 Serological diagnostic tests**

Detection of antibodies or virus-specific antigens against the SARS-CoV-2 virus are important alternatives for the diagnosis of the disease and monitoring the spread of the

virus. The use of these tests are needed for urgent medical diagnosis which is difficult to access the molecular tests (Lin, D., et al., 2020).

### **1.3.2.1 Antigen detecting diagnostic tests**

Antigen detection tests are based on detecting the presence of viral components in respiratory tract samples that are expressed during infection by SARS-CoV-2.

In a study done in Japan, the SARS-CoV-2 genome was transcribed and then RNA was converted to cDNA, coding regions were amplified and cloned into the pET30a vector. The recombinant full-length N antigen was expressed in engineered *Escherichia coli*. N antigen was purified using BL21 strains and Ni-NTA resin. Magnetic beads Magnosphere™ MS300 were used in this study. Recombinant N antigens were coupled to these tosyl magnetic beads using the catalytic reagent solution according to the manufacturer's instructions, and the resulting beads were further blocked with 0.05% BSA for 6 hours at 37 °C. The applied test and detection procedure was automated on a chemical immunoluminescence analyzer ACCRE6. Fifty microliters of pure plasma was first incubated with antigen-coupled magnetic beads at 37 °C for 5 minutes. Unbound material was then gently removed and then washed three times with Tris buffer. Alkaline phosphatase-labeled antihuman immunoglobulin (50 µg/mL) was added and incubated for an additional 5 minutes at 37 °C in MES buffer. After three washes to remove unbound material, Lumigen APS-5 substrate (50 µg/mL) was added. As a result, the light signal was measured in relative light units by the photomultiplier in ACCRE6, and the entire test can be completed in 23 minutes. The sensitivity and specificity of the test depend on several factors, such as the disease stage, viral load, and specimen quality (Lin, D., et al., 2020).

### **1.3.2.2 Antibody diagnostic tests**



Antibodies, also called immunoglobulins, are Y-shaped proteins. When a foreign substance (antigen) enters the body, it is produced by the immune system and then these molecules bind to the foreign substance and neutralize it. Antibodies are weapons used by the immune system to fight new infections (Togay A. and Yılmaz N., 2020).

Detection of IgM, IgA, IgG and total antibodies reflecting the host immune response developed during infection constitutes a wide range of tests. Antibody development is largely dependent on the state of the host immune system; It is affected by age, nutrition, use of immunosuppressive drugs and concomitant diseases (De, D., Pandhi, D., 2020).

Clinically, SARS-CoV-2 specific IgA and IgM were detected 7 days after virus infection and 3-4 days after onset of symptoms. The specific IgG of the virus appears 7-10 days after SARS-CoV-2 infection (Cai, X. F., et al., 2020)

The ELISA test is based on coloring the reaction using enzyme-labeled conjugate and enzyme substrate to show the specific antigen-antibody reaction. Currently, the enzyme-linked immunosorbent assay (ELISA), colloidal gold immunochromatographic assay (CLIA) are the most preferred methods for detecting SARS-CoV-2. Antibody-base methods targeting IgG and IgM produced against recombinant N and S proteins of SARS-CoV-2 are consistent with results obtained with nucleic acid-based methods. As a result of these studies, it was found that the receptor binding domain (RBD) of the viral S protein of the SARS-CoV-2 virus showed better antigenicity than the viral Nucleocapsid protein for the diagnosis of SARS-CoV-2 infection. In addition, a recent report indicates that the level of IgA in patient serum is positively correlated with the severity of COVID-19, furthermore, the identification of IgA in serum indicates that it can also be used as a biomarker for COVID-19. The sensitivity of IgG and IgM targeted methods is over 71.4% and 57.2%, and even their sensitivity increases to 97.5% and 87.5%, respectively. Specifically, the sensitivities of RBD-specific IgA, IgM, and IgG were 98.6%, 96.8%, and 96.8%, respectively, and the sensitivities of RBD-specific IgA, IgM, and IgG were 98.1%, 92.3%, and 99.8%, respectively (Li, C., and Ren, L. (2020).

The positive result of the serological test performed to detect IgA and IgM antibodies against COVID-19 infection indicates that the person has recently encountered the virus. Positive detection of IgG antibodies in the test indicates exposure to COVID-19.

This antibody usually reaches positive levels within 10 days after the first symptoms start. The indicator of understanding the person's response to the virus with the immune system is a positive response of the IgG antibody. This result becomes even more important in determining people who have had the disease asymptotically (Togay A. and Yılmaz N., 2020). Multiple samples can be examined simultaneously with RT-PCR and ELISA testing.

However, trained personnel and laboratory equipment are required to carry out these tests. The tests duration is approximately 1 hour.

#### **1.4 Lateral Flow Test (LFT) Based Diagnosis**

The specificity of SARS-CoV-2 N gene regions has potential to be adapted to various identification methods including immunochromatographic tests. The first type of LFT is the pregnancy test (O'Farrell, B., 2009). Due to the bacterial and virus infections caused by COVID-19 and various epidemics the development of rapid point-of-care tests such as LFTs are always needed.

These tests have many advantages compared to the other detection methods, such as being fast, simple, robust and cost-effective. LFT results can be observed with the naked eye and efficient test platform is being developed (Sajid, M., et al., 2015). Basically, it is easy to use diagnostic device used to verify the presence or absence of a target analyte in humans or animals, such as pathogens or biomarkers or contaminants in water sources, foodstuffs or animal feed. Due to their versatile structure of LFT is used in pharmaceutical, environmental, animal health, food and feed test, plant and product health (Kaya, E., et al., 2014). LFTs are usually produced in strip form. It is often 4-6 mm in width, 6-7 cm in length, and 1-2 mm in thickness. These dimensions are generally similar as it operates according to the capillary flow principle.

The remarkable parts of the structure of the immunochromatographic card tests are generally listed below.

1. Plastic base and cassette cover.
2. Cellulose-made sample pad where the sample is dropped.
3. Fiber glass structured reaction pad containing colored molecules and antibodies and where reactions take place.

4. Nitrocellulose membrane where capillary current takes place and the result is monitored.
5. Test line and control line.
6. Cellulose-made waste pad where the remaining sample accumulates (Kaya, E., et al., 2014).

In general, LFT consists of 4 basic materials. These materials are; sample pad, conjugate pad, absorbent pad and nitrocellulose membrane. LFT works on the principle of capillary flow. The sample solution dropped on the sample pad passes through the conjugate pad and moves towards the nitrocellulose membrane(NCM). If the target sequence is present in the sample solution with the test and control line on the NCM, it hybridizes. Excess sample solution advances through the absorbent pad and the excess accumulates on the absorbent pad (Kaya, E., et al., 2014). Figure 1.2 shows that schematic representation of the LFT.

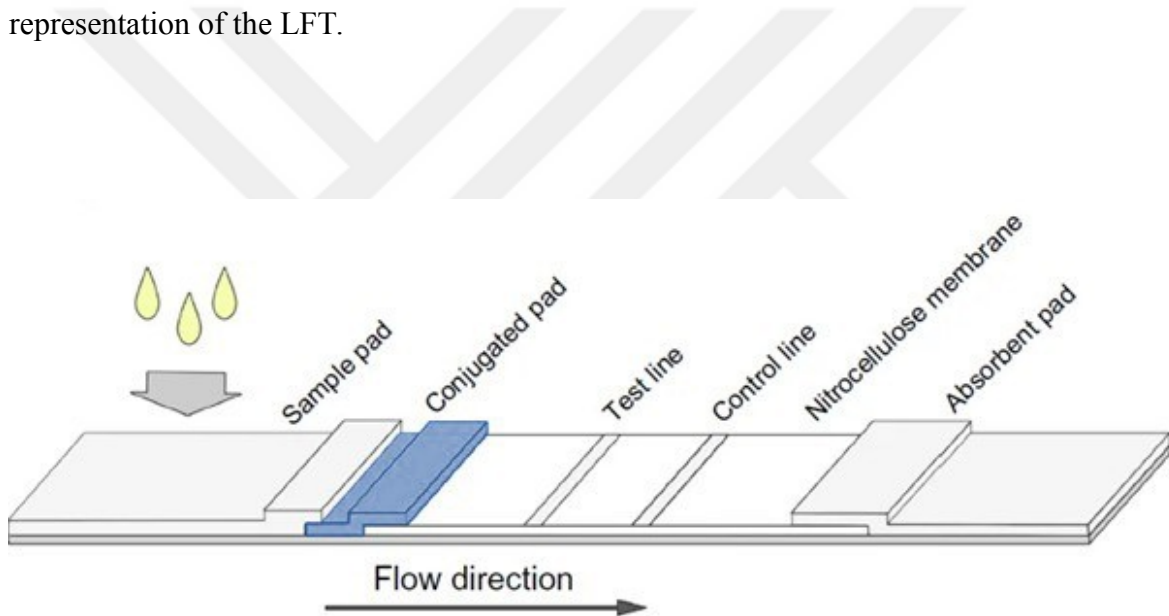


**Figure 1.2 :** Schematic representation of the lateral flow test (Wang, Z., et al., 2014).

The pH adjusted and buffer pretreated sample is applied to the sample pad. If there is a target (antibodies, nucleic acids) in the applied sample solution, the test line is bound to the detection probe. The target detection probe mix moves across the nitrocellulose membrane, and then the complementary probe reacts with the target molecule and is captured in the control line. The formation of a colored line visible to the naked eye on the test line and control line indicates a positive result.

A number of LFTs were developed for the diagnosis of COVID-19. Although antibody and nucleic acid based LFTs are announced most of them are based on antibody

detection caused by SARS CoV-2. For instance they have been developed specifically for antibodies produced against N, S and Orf3a proteins SARS-CoV-2. Interestingly, no antibodies were detected to E protein.

The diagnostic indexes of LFT-based IgM/IgG tests were demonstrated at different time points after onset of the symptoms, where in at 0–7 days, 8–15 days and 16 days or more after symptom onset these tests showed 18.8%, 100% and 100% sensitivity and 77.8%, 50% and 64.3% specificity, respectively. Additionally, IgM and IgG based LFT was also developed by using the recombinant RBD domain of S protein of SARS CoV2. Results interpreted with both IgM and IgG bands showed 88.66% sensitivity and 90.63% specificity which were better than single IgM and IgG tests. A study in the United States with defined cases estimated 91.8% sensitivity and 99.5% specificity (Ejazi, S. A., et al., 2021). In terms of the nucleic acid based LFTs for SARS CoV2, the test principle depends on the CRISPR based method and needs the complex and expensive experimental steps (Broughton, J. P., et al., 2020, Xiong, D., et al., 2020).

### **1.5 Aim of the Study**

This study aims to develop a detection platform for the N gene region of SARS-CoV-2 that causes COVID-19 using AuNP based LFT. For this purpose, two types of sandwich models for the detection of different sized N gene regions were designed and applied to the assay.

## **2. MATERIALS AND METHODS**

## **2.1 Materials**

### **2.1.1 Chemicals and reagents**

The chemicals used in this study were all analytical grades. Gold(III) chloride trihydrate was purchased from (Alfa Easar), and Sodium citrate dihydrate (Thermo fisher), Tris-HCl (Applichem), KCl-NaCl (Merck), MgCl<sub>2</sub>-CaCl<sub>2</sub>-SSC (Multicell), Tween-20 (Biofrox), TCEP (Sigma Aldrich), Gene Ruler 100bp DNA ladder-Ultra Low Range DNA ladder-10X Reaction buffer-Tag DNA polymerase (Thermo Scientific), 6X loading dye (Fermentas), Nuclease free water (Promega) were also used in this study. Ultrapure water was used for the preparation of all solutions during the study. The nitrocellulose membrane cards were purchased from Whatman, Germany, and absorbent pad, sample pad and conjugate pad were purchased from Millipore, USA.

### **2.1.2 Buffers and solutions**

A few buffer solutions were prepared and used for LFTs optimizations. The list of experienced buffers is given in Table 2.1.

**Table 2.1 : Buffer tables**

10X PBS (20mL)	50mM NaCl	5mM KCl	20mM Na <sub>2</sub> HPO 4	KH <sub>2</sub> PO <sub>4</sub>			
Sodium Phosphat e Buffer (50mL)	20mM NaH <sub>2</sub> PO 4	Na <sub>2</sub> HPO 4	BSA	0.25 %Tween- 20	10 %Sucros e		
No. 14 Running Buffer (10mL)	20mM Tris	50mM NaCl	5mM KCl	MgCl <sub>2</sub>	CaCl <sub>2</sub>	0.1M m BSA	Triton -X 100
No 4. Sample Pad Buffer (10mL)	0.05M Tris-HCl	Triton-X 100	0.15M NaCl				
No. 5 Sample Pad Buffer (10mL)	0.1mM NaCl	0.2 %Tween- 20	PBS				

### 2.1.3 Test strip components

Strip cards have four components. They are nitrocellulose membrane (Whatman 1 and Whatman 2) as a main reaction material, glass fiber pads as a conjugate pads and cellulose fiber pad as a sample application pad and absorbent pad.

#### **2.1.4 Synthetic oligonucleotides**

All modified and unmodified synthetic oligonucleotides for target hybridization and universal PCR primers were purchased from Integrated DNA Technologies (IDT) and were dissolved in nuclease-free water then stored at -20°C. A target sequence of 72 and 50 bases in length from the N gene of the SARS-CoV-2 virus was selected for optimization studies and also purchased from IDT. As a negative control running buffer, SE-20-60 aptamer and ORF 1ab was used for selectivity. Table 2.2 demonstrates the used sequences and primer sets in this study.

**Table 2.2** : Sequences and modifications of synthetic probes for N gene detection

Synthetic target 1 (72bp)	5'-GGG AGC CTT GAA TAC ACC AAA AGA TCA CAT TGG CAC CCG CAA TCC TGC TAA CAA TGC TGC AAT CGT GCT ACA-3'
Probe 1	5' TTT GGT GTA TTC AAG GCT CCC AAA AAA AAA-3 -SH'
Detection probe 1 (TL)	5'bio AAA AAA TG CGG GTG CCA ATG TGA TCT 3'
Complementary probe 1 (CL)	5' GGG AGC CTT GAA TAC ACC AAA TTT 3'bio
Synthetic target 2 (50bp)	5' AAT ACA CCA AAA GAT CAC ATT GGC ACC CGC AAT CCT GCT AAC AAT GCT GC -3'
Probe 2	5' T GCC AAT GTG ATC TTT TGG TG AAA AAA AAA-3 -SH
Detection probe 2	5'bio AAA AAA GC AGC ATT GTT AGC AGG ATT 3'
Complementary probe 2 (CL)	5' CA CCA AAA GAT CAC ATT GGC A TTT 3'bio
Negative control 1: SARS-CoV-2 ORF 1ab	CCC TGT GGG TTT TAC ACT TAA ACG ATT GTG CAT CAG CTG ACC CTG TGG GTT TTA CAC TTA AAA ACA CAG TCT GTA CCG TCT GCG GTA TGT GGA AAG GTT ATG GCT GTA GTT ATA ATC AAC TCC GCG AAC CCA TGC TTC AGT CAG CTG ATG CAC AAT CGT
Negative control 2: SE-20-60-	5'Bio CTC CTC TGA CTG TAA CCA CGC ACA AAG GCT CGC GCA TGG TGT GTA CGT TCT TAC AGA GGT-3'
Forward primer :	GGG AGC CTT GAA TAC ACC AAA A
Reverse primer :	TGT AGC ACG ATT GCA GCA TTG

## 2.2 Methods

### 2.2.1 Gold nanoparticle synthesis



Gold nanoparticles (AuNPs), approximately 20 nm in diameter, were prepared by reducing H<sub>2</sub>AuCl<sub>4</sub> with sodium citrate (Grabar, K. C. et al, 1995). All the glass materials used in the synthesis of AuNPs were cleaned with acid solution. It was rinsed with pure water and used after drying. Briefly, 100 mL of 1mM H<sub>2</sub>AuCl<sub>4</sub> solution was boiled by stirring continuously with magnetic stirrer. Then 1% sodium citrate was added. After 2-3 minutes the color of solution turned from black to red, boiling was continued for 10 minutes and finally the solution was allowed to cool room temperature. AuNP solution was filtered through a 0.45 μm acetate membrane filter before using. AuNP solution was four time concentrated (4X) for oligonucleotide conjugation by centrifugation at 3750 rpm at 10°C for 30 minutes using Amicon Ultra centrifuge tube.

#### **2.2.1.1 Conjugation of AuNPs with thiolated oligo probes**

Conjugation of 5' thiolated DNA probes with AuNPs was performed. Before starting the conjugation, tris(2-carboxyethyl)phosphine (TCEP) was used to break the disulfide bonds in the probes (probe 1 and probe 2 given the Table 2.2) and activated for oligonucleotides binding. Briefly, 10 μM TCEP and 100 μM thiolated probes were incubated for 1 hour. Then oligonucleotides were added to the 4-fold concentrated AuNP solution and incubated for overnight at room temperature..

After the incubation, the resulting conjugate was aged slowly by adding 0.1 M phosphate buffered saline (PBS) and incubated at 4°C. Excess reagents were removed by centrifugation at 12000 rpm for 30 minutes, and after discarding the supernatant, the pellet was washed with sodium phosphate buffer at two times. After the centrifugation pellet was resuspended in 20 mM sodium phosphate buffer containing 5% BSA, 0.25% Tween20, and 10% sucrose and stored at 4°C.

#### **2.2.2 Preparation of test components**

The LFT strip consists of four components: sample application pad, conjugation pad, absorbent pad, and nitrocellulose membrane. Each component was prepared separately and then combined. The sample applied was soaked with Tris buffer containing 0.25% Triton X-100 and 0.15 M NaCl before use and dried at 37° for 1 hour.

The conjugate pad was soaked with of AuNP-DNA conjugates and dried at 37° for 1 hour. Absorbent pad was used without any treatment.

Complementary probe and detection probes were immobilized on the nitrocellulose membrane using micropipette manually in the principle of the interaction of biotin-streptavidin to create the visible lines in each strip. Shortly, 1 mg/mL of streptavidin and 100 µM biotinylated probe were mixed and incubated for 1 hour. Then it was centrifuged at 14000 rpm for 15 minutes using with an ultra centrifugal tubes and washed with PBS for two times. Finally, remaining part was added with PBS and store at -20°C. Then 0.6 µL conjugated oligonucleotides were dispensed onto the NCM as a test and control line by pipetting.

### **2.2.3 Assembly of lateral flow test strip**

When assembling the test strip, the sample pad, conjugate pad, nitrocellulose membrane, and absorbent pad were cut into 0.4 cm dimensions and overlapped together.

### **2.2.4 PCR conditions for N protein sequence**

The sequence of the 72 base long N sequence was amplified by PCR and applied to LFT. PCR mix was prepared in 50  $\mu$ L volume and conditions were given in Table 2.3 and Table 2.4.

**Table 2.3 : PCR Conditions for 72bp of N gene**

Steps	Conditions	
Initial Denaturation	95°C, 3 minutes	
34 cycles	Denaturation	95°C, 30 seconds
	Annealing	54°C, 30 seconds
	Extension	72°C, 15 seconds
Final Extension	72°C, 4 minutes	

**Table 2.4 : Optimized PCR conditions for 72 bp amplicon**

Component	Final Concentration
ddH <sub>2</sub> O	-
10X Reaction Buffer	1X
2mM dNTP Mix	0.2 $\mu$ M
10 $\mu$ M Forward Primer	0.5 $\mu$ M
10 $\mu$ M Reverse Primer	0.5 $\mu$ M
121,7 ng/ $\mu$ L DNA Template	2.43ng/ $\mu$ L
5 U/ $\mu$ L Taq Polymerase	0.05U
25mM MgCl <sub>2</sub>	2Mm

### 2.2.5 Agarose gel electrophoresis of PCR products

2% agarose in 25 mL of 1X TAE buffer was prepared and added with 2.5  $\mu$ L of ethidium bromide. PCR amplicons were loaded into the gel by mixing with 6X Orange dye and GeneRuler Ultra Low Range (ULR) and GeneRuler 100bp ladder were used as DNA marker. The gel was run for 45 minutes at 90V and visualized with the SYNGENE G:BOX UV gel imaging system.

### **2.2.6 Assay procedure for the synthetic target**

Both the synthetic target and negative controls were diluted in 100  $\mu$ L of 5X SSC as 1  $\mu$ M final concentration and applied to the sample pad. As a negative control, 100  $\mu$ L of 5X SSC was also applied. The applied samples were allowed to pass through the nitrocellulose membrane and reach the absorbent pad. Strip test were then washed with 50  $\mu$ L of 5X SSC.

### **2.2.7 Assay procedure for PCR products**

Amplified amplicons of the SARS-CoV-2 N gene 72 bp were applied to the LFT. Prior to administration, amplicons were incubated for 5 minutes at 95°C for denaturation. ORF 1ab amplicons were used as negative controls. Both the target and negative control sequences were diluted in 5X SSC as a ratio of 1:10 and loaded into the strips in 100  $\mu$ L volume and washed with 50  $\mu$ L of 5X SSC.

### **2.2.8 Hybridization models used in LFT**

Two different hybridization models were used in LFT strip studies. These models hybridize specifically to sequences in the conserved region of the N gene of SARS-CoV-2. Model 1 and Model 2 were designed specifically for the WHO-approved conserved N3 sequence of the N gene. Model 1 is for 72 base long, while model 2 is for 50 base long. Since these sequences were designed specifically for conserved regions in the N gene, they were successfully used in the LFT. Figure 2.1 shows hybridization models.

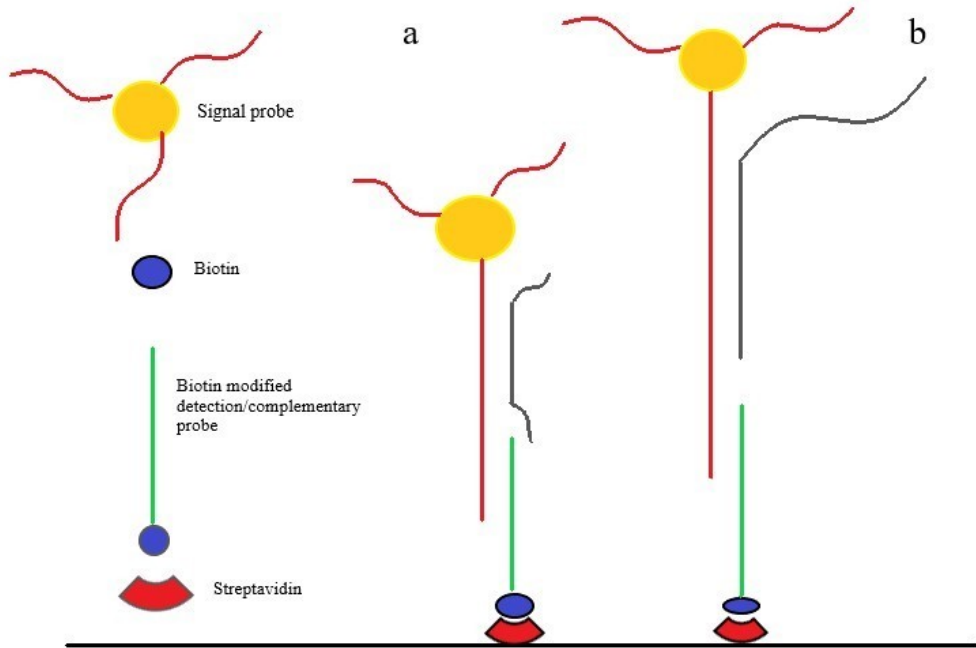


**Figure 2.1 :** Plot of detection of target nucleic acids by sandwich hybridization. a and b represent 50 base long synthetic target and 72 base long synthetic target, respectively.

### 3. RESULTS AND DISCUSSION

#### 3.1 Synthesis of Gold Nanoparticles

Gold nanoparticles (AuNPs) with an average diameter of about 20 nm were synthesized by the citrate reduction method (Grabar, K. C. et al, 1995). The sizes and shapes of AuNPs directly affect their optical properties. Because of these properties, the synthesized AuNPs are characterized by analysis of their absorption maxima. Spherical colloidal AuNPs have an average absorption between 500 nm and 570 nm. While the smaller AuNPs have an absorption close to 520 nm larger have peaks near to longer wavelengths. If AuNPs are aggregated, the optical properties and absorption patterns change significantly. Therefore, UV-visible spectroscopy is used to monitor the stability of particles. Figure 3.1 shows the maximum absorption peak of synthesized AuNPs (A) and synthesized and concentrated AuNPs (B).

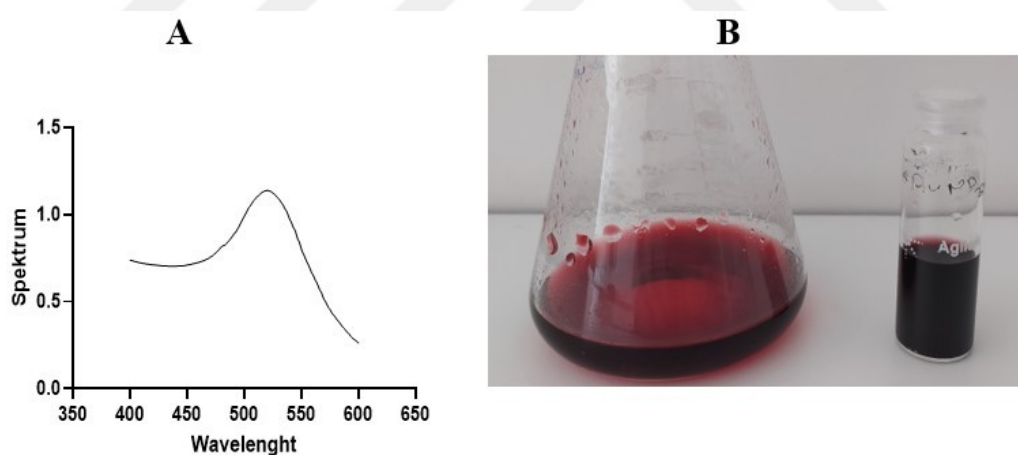


**Figure 3.1** : UV-Vis Spectrum of synthesized AuNPs (A) and 4X concentrated AuNPs (B)

Results showed that the spectrum pattern and maximum absorption,  $\lambda_{\max}$  was observed at 521 nm as expected. This also indicates the pure, unprecipitated and stable state of colloidal AuNPs.

### 3.2 Functionalization of Conjugate Probes

Probes were dissolved in distilled water as 100 $\mu$ M stock concentrations. Then probes were prepared as 2  $\mu$ M, 4  $\mu$ M and 8  $\mu$ M for conjugation as final concentration for model 1 and model 2.

Since the molecular charge of DNA and AuNPs is negative, electrostatic repulsions prevent DNA-AuNP conjugation. To avoid this problem and increase the conjugation capacity, the solution containing the activated probe and AuNPs was salt-aged with PBS.

After salt aging, excess salt and probes were removed from the solution by centrifugation and the remaining pellet was suspended in 20 mM phosphate buffer containing 5% BSA, 0.25% Tween20 and 10% sucrose. Figure 3.2 demonstrates the prob-AuNP conjugation before and after salt aging.

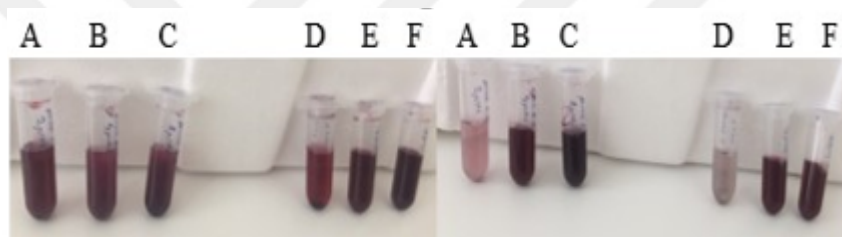


**Figure 3.2 :** AuNP-Probe conjugations for model 1(A-B-C) and model 2 (D-E-F). Left side before salt aging (A-B-C-D-E-F) and right side after salt aging (A-B-C-D-E-F).

Results show that electrostatic impulses are eliminated, and conjugation capacity is increased. Since the 2  $\mu$ M prob concentrations caused aggregation of AuNPs (A,D) for two types of models, 4  $\mu$ M and 8  $\mu$ M probs (B,C and E,F) were used for further experiments as they stabilize the AuNPs and do not show the flocculation.

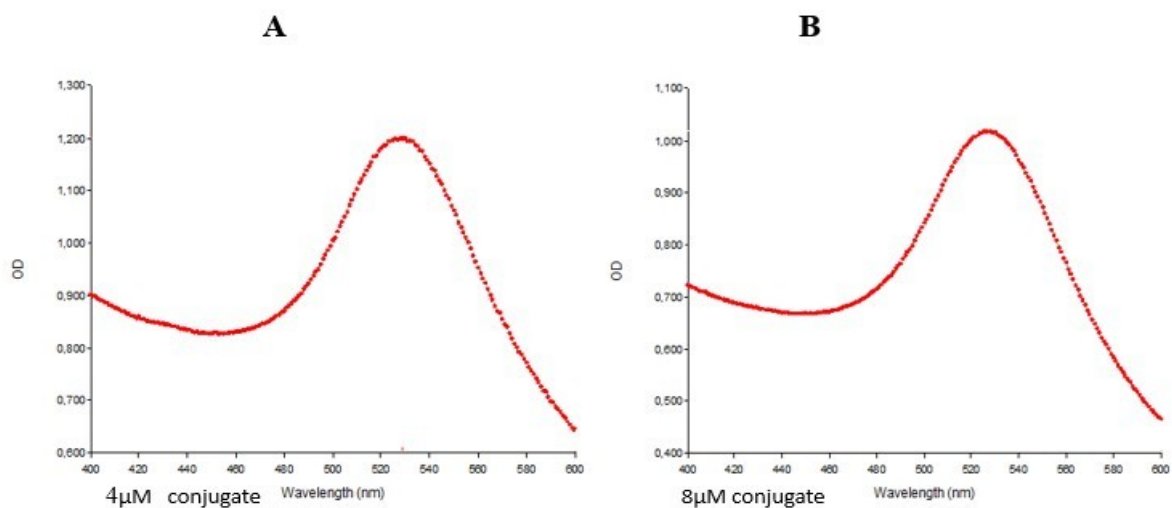


**Figure 3.3 :** Absorption spectrum of 4μM(A) and 8μM(B) oligo conjugate of model 1.

Result shows that after the conjugation of 4μM probe,  $\lambda_{\max}$  of naked AuNPs changed from 521 nm to 529 nm (A) and 526 nm (B) after the conjugation of 8μM probe 1. The increase in  $\lambda_{\max}$  values in both conjugates indicates successful binding of oligonucleotides on AuNP.

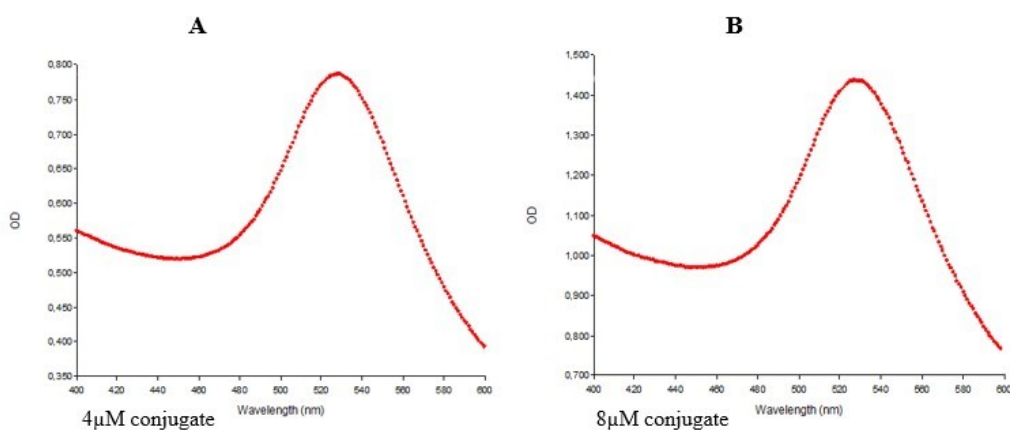


**Figure 3.4 :** Absorption spectrum of 4μM(A) and 8μM(B) oligo conjugate of model 2.

Result shows that after the conjugation of 4 μM prob 2,  $\lambda_{\max}$  of naked AuNPs changed from 521 nm to 527 nm (A) and 528 nm (B) after the conjugation of 8 μM prob 2.



The increase in  $\lambda_{\max}$  values in both conjugates indicates the successful binding of oligonucleotides on AuNPs.

While the naked AuNPs have a wavelength of 521 nm, the wavelength of the prob 1 conjugate for 4 $\mu$ M (529 nm) and 8 $\mu$ M (526 nm) and prob 2 conjugate for 4 $\mu$ M (527 nm) and 8 $\mu$ M (528 nm) is higher than the synthesized AuNP. Thus, this indicates that oligo-AuNP conjugations were successfully performed. As expected, stability was achieved by 4 $\mu$ M and 8 $\mu$ M concentrations and future experiments were continued with these concentrations since there was no precipitation.

### 3.3 N Gene PCR

The N3 region of SARS-CoV-2 was amplified by PCR (Figure 3. 5) and used as target in LFT.

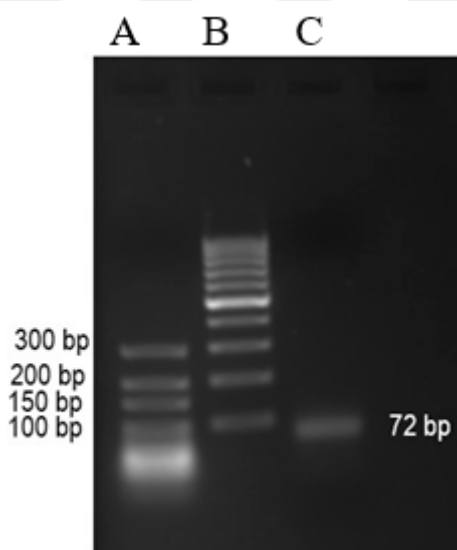


**Figure 3.5 :** Agarose gel image of PCR product. A) Ultra Low Range DNA ladder. B) 100 BP DNA ladder. C) N gene product.

### 3.4 The Working Principle of LFT

The working principle of nucleic acid-based LFT is that if the sample applied to the sample pad contains the target sequence, it partially hybridizes to the AuNP-probe complex present in the conjugation pad. After that it will be captured by detection probe present on the test line on the NCM via hybridization. A red line originating from AuNP appears on the test line. The excess amount of conjugate makes hybridization by complementary probe present on the control line on NCM. The formation of a red line on the test line indicates that the analyte is present in the sample and test is positive.

A red line on the control line also indicates that the test is working successfully. If there is no line on the control line, the test is invalid.

### 3.5 Temperature Optimization Experiments

SARS-CoV-2, N gene specific synthetic oligonucleotide was applied to LFT. Target was brought to final concentrations of 1  $\mu\text{M}$  with 5X SSC. As a negative control 5X SSC was used and strips were washed with 5X SSC. Temperature optimization was done using Whatman 2 (Figure 3.6) and Whatman 1 membranes (Figure 3.7) for model 1.

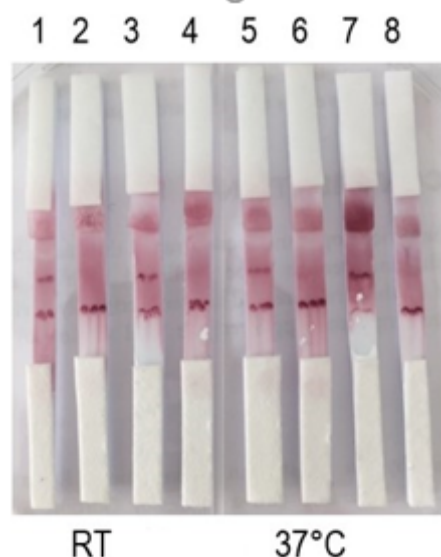


**Figure 3.6 :** Temperature optimization for LFTs using Whatman 2 membrane. Strips 1-3-5-7 were applied with 1  $\mu\text{M}$  target analyte in 5X SSC and strip 2-4-6-8 were applied with 5X SSC as a negative control. Strip 1-2-5-6 have 4  $\mu\text{M}$  probe, strip 3-4-7-8 have 8  $\mu\text{M}$  probe experiments. RT: Room temperature. Sample pad buffer no.4 was used for the sample pad.

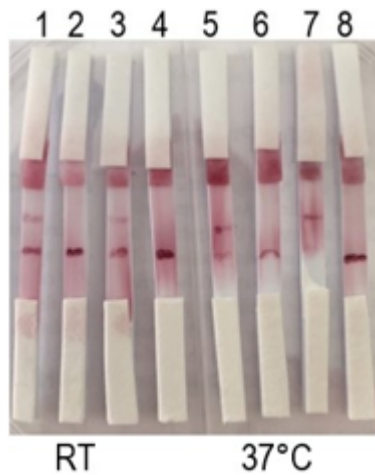


**Figure 3.7 :** Temperature optimization for LFTs using Whatman 1 membrane. Strips 1-3-5-7 were applied with  $1\mu\text{M}$  target analyte in 5X SSC and strip 2-4-6-8 were applied with 5X SSC as a control. Strip 1-2-5-6 have  $4\mu\text{M}$  probe, strip 3-4-7-8 have  $8\mu\text{M}$  probe experiments. RT: Room temperature. Sample pad buffer no.4 was used for the sample pad.

The results in Figure 3.6 and 3.7 show that RT and  $37^\circ\text{C}$  have no significant result in terms of the line intensity. However, drying at  $37^\circ\text{C}$  have a little more efficiency in the flow rate and the binding of AuNP in the conjugate pad. Additionally, Whatman 2 membrane seems better than Whatman 1 for model 1 at  $37^\circ\text{C}$ . Therefore, strip preparation was performed at  $37^\circ\text{C}$  for further experiments with Whatman 2 membrane for model 1. There were also no significant differences for the probe concentration ( $4\mu\text{M}$  -  $8\mu\text{M}$ ) in terms of the flow and line intensity (Figure 3.6).

### 3.6 Buffer Optimization Experiments

Buffers have a significant effect on LFTs. Since they cause nonspecific binding or prevent the efficient flow 3 types of running buffer and 2 types of sample pad buffer were experienced for model 1 optimization using Whatman 2 membrane and 4 $\mu$ M (Figure 3.8) and 8  $\mu$ M probe (Figure 3.9). They are No.14, 5X SSC, 1X PBS as a running buffer and sample pad no.4 and sample pad no.5 as a sample pad buffer.

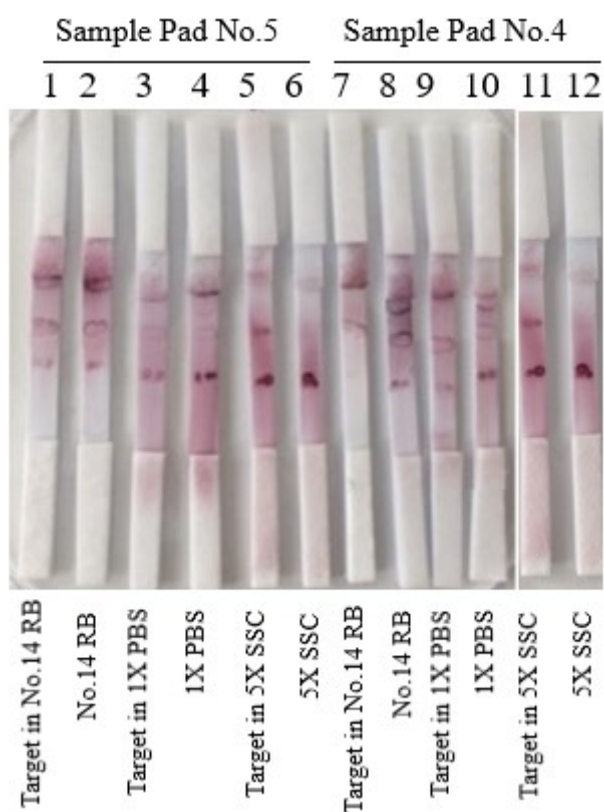


**Figure 3.8** : Buffer optimization for LFTs using 4 $\mu$ M of model 1 . Buffers were applied as alone and with the target. Strips 1-3-5-7-9-11 contain 1 $\mu$ M target. Strips 2-4-6-8-10-12 are only buffers. RB: Running buffer. 5X SSC used as a negative control.

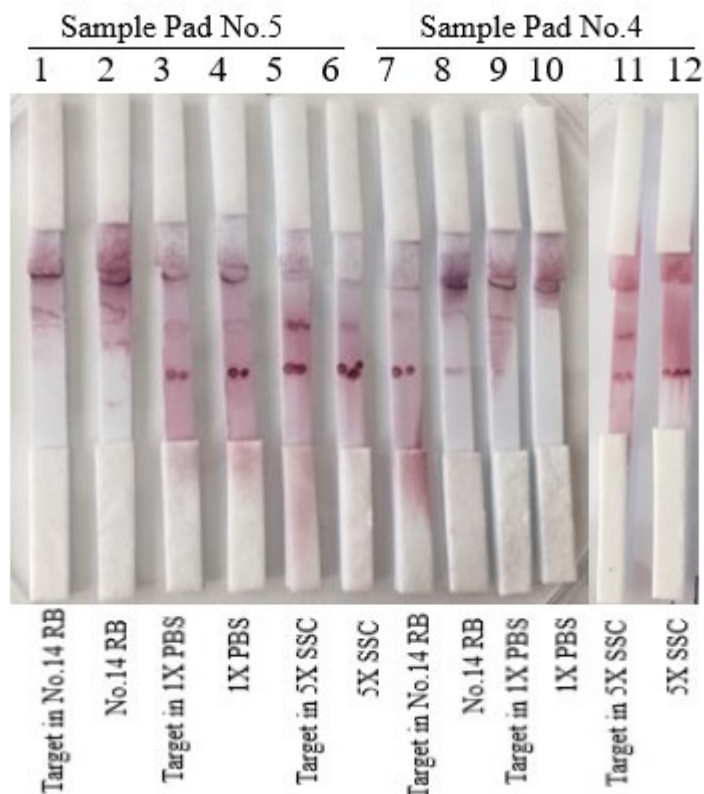


**Figure 3.9** : Buffer optimization for LFTs using  $8\mu\text{M}$  of model 1 . Buffers were applied as alone and with the target. Strips 1-3-5-7-9-11 contain  $1\mu\text{M}$  target. Strips 2-4-6-8-10-12 are only buffers. RB: Running buffer. 5X SSC used as a negative control.

In the Figures 3.8 and 3.9,  $4\mu\text{M}$  and  $8\mu\text{M}$  conjugates were applied in running buffer using Whatman 2 membrane and sample pads 4 and 5. It was continued with 5X SSC as a running buffer because it did not show non-specific binding and the flow rate was appropriate (Figure 3.8, strip 6,12; Figure 3.9 strip 12). Therefore, sample pad no.4 was selected for further studies. Because it gave better line intensity, test and control lines were prominent, and flow was not affected negatively.

### 3.7 LFT for PCR Product

N gene region amplified by PCR was applied to LFTs strips prepared on Whatman 2 membrane in 5X SSC as a running buffer. Figure 3.10 shows the PCR product experiment on LFTs. According to the results, the N gene region amplified by PCR was detected by LFT successfully and selectively and it did not show the nonspecific binding to the ORF 1ab sequence as expected. This means that model 1 is suitable for selective hybridization in the LFT.

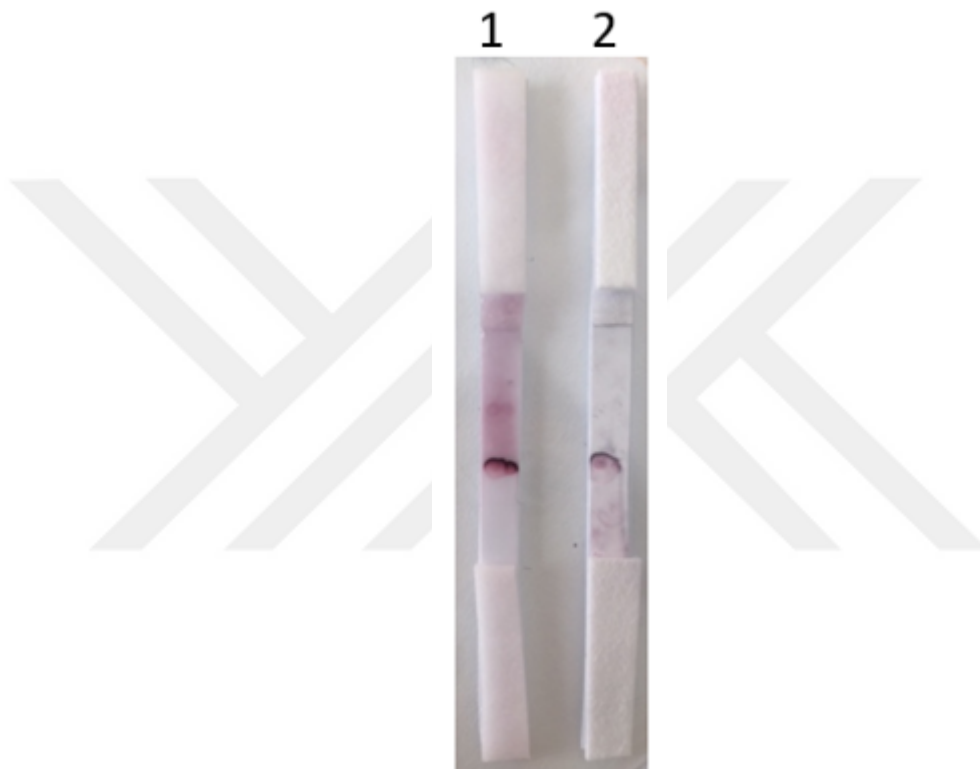


**Figure 3.10 :** Application of PCR product of N3 gene region to LFT using Whatman 2 membrane with model 1. 5X SSC buffer and sample pad no.4 was used in the assay. ORF 1ab sequence was used as negative control.

### 3.8 Result of Model 2

50 base long target application is shown in Figure 3.11.

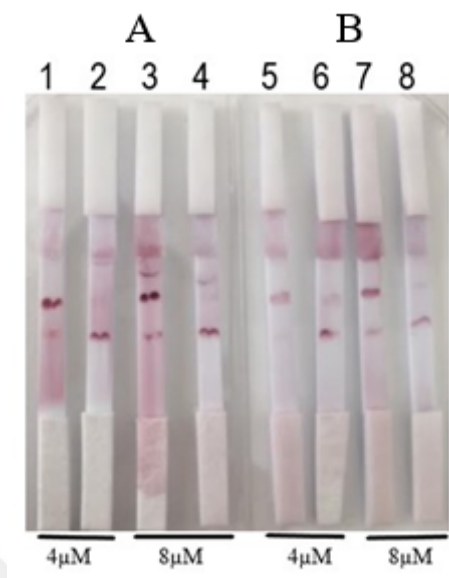
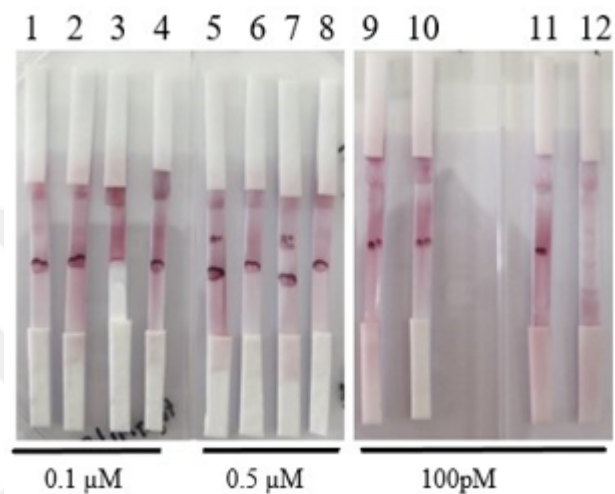


**Figure 3.11** : LFT strip assay developed by two models. Strips 1-4 were developed by Whatman 2(A) membranes and strips 5-8 were developed by Whatman 1(B) membranes. 5X SSC was used as RB. 1 $\mu$ M target was loaded on the strips 1,3,5,7. Strips 2,4,6,8 are negative controls applied with 5X SSC buffer.

According to the results in Figure 3.11, nonspecific binding was not observed in LFT with Whatman 2 membrane. However, nonspecific binding was detected in the Whatman 1 membrane using 4  $\mu$ M and 8  $\mu$ M strip (6,8). Therefore, further studies were performed by Whatman 2 membrane for two probe concentrations (Strip 1-4).

### 3.9 Limit of Detection

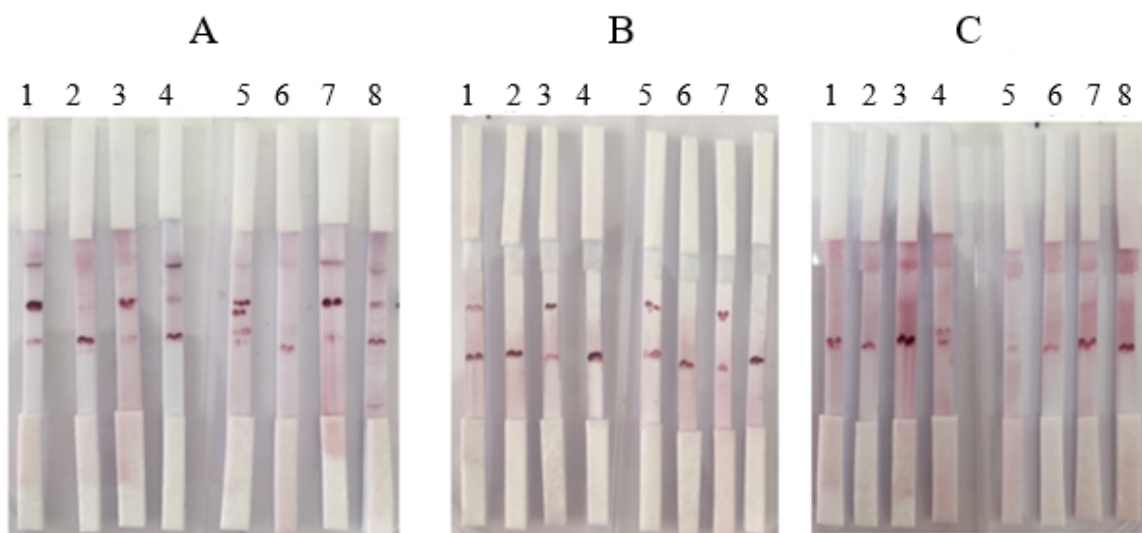
Limit of detection (LOD) of LFT for SARS-CoV-2 detection was performed by using synthetic target with Whatman 1 membrane and Whatman 2 membrane. Both 4  $\mu\text{M}$  and 8  $\mu\text{M}$  probs were used. Sample pad no. 4 was used in all LOD experiments. 5X SSC was used as RB and experiments were performed by 4 $\mu\text{M}$  and 8  $\mu\text{M}$  probe 1 and probe 2. The detection limit results were given in Figure 3.12, 3.13, 3.14, and 3.15.



**Figure 3.12 :** Limit of detection experiments using Whatman 2 membrane with Model 1. Strips 1,2,5,6,9,10 contain 4 $\mu\text{M}$  probes 1, strips 3,4,7,8,11,12 contain 8 $\mu\text{M}$  probes 1. Strips 1-4 contain a 0.1 $\mu\text{M}$  target, strips 5-8 contain a 0.5  $\mu\text{M}$  target, and strips 9-12 contain a 100pM target. 5X SSC was used as RB and negative control.

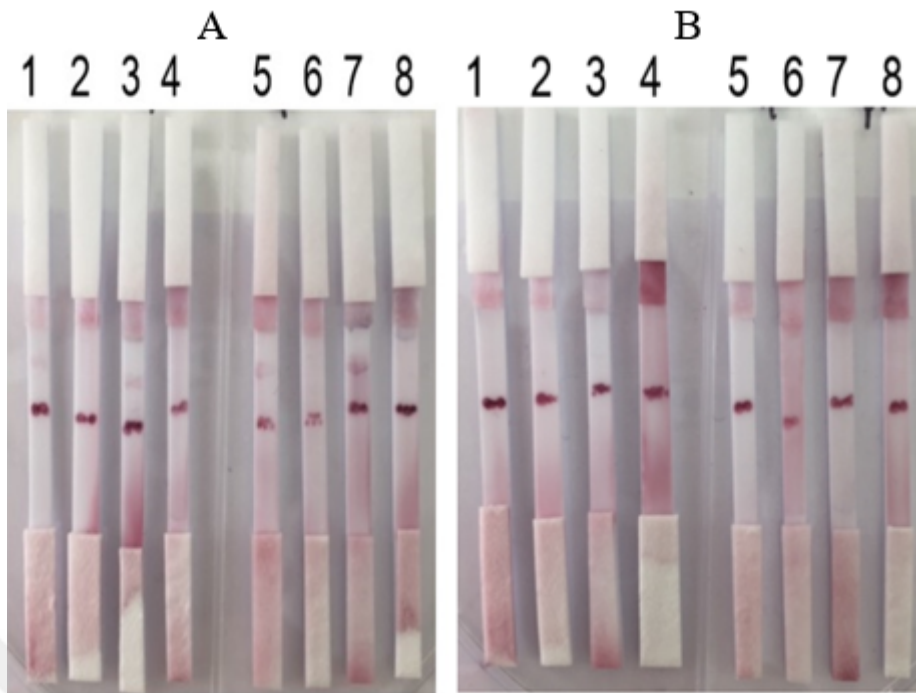
Figure 3.12 results showed that the LOD is detected by 4  $\mu\text{M}$  and 8  $\mu\text{M}$  probs 1 as 0.5  $\mu\text{M}$  (strip 5,7). These strips were developed by Whatman 2 membrane with Model 1.





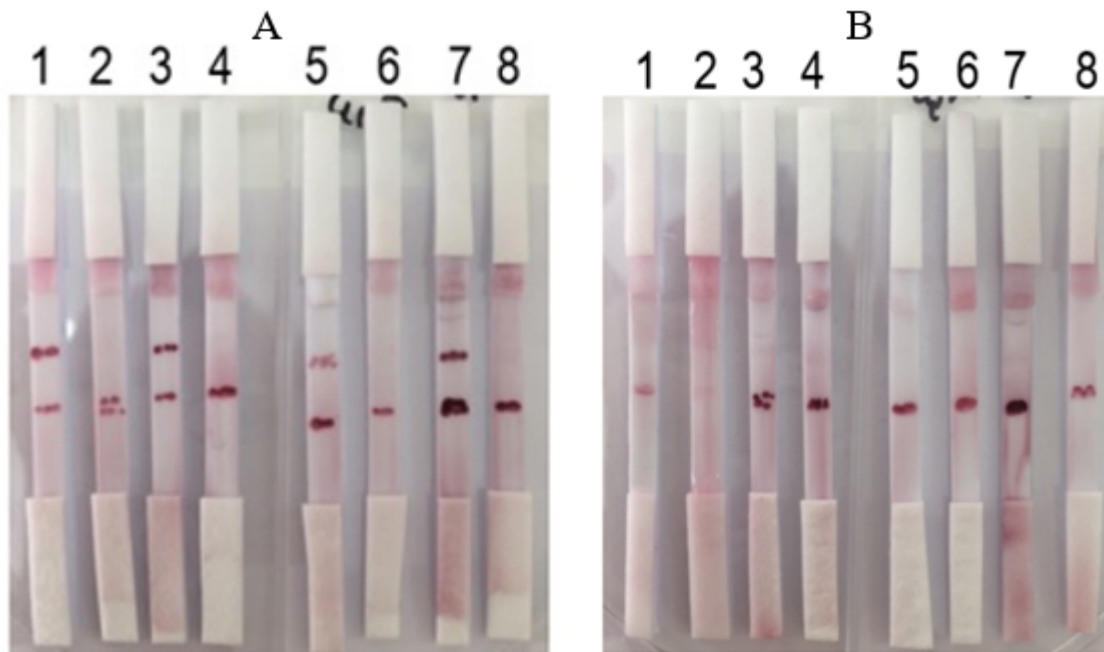
**Figure 3.13** : Limit of detection experiments using Whatman 2 membrane with Model 2 (A-B-C). Strips 1,2,5,6 contain 4 $\mu$ M probe 2, strips 3,4,7,8 contain 8 $\mu$ M probe 2. A) Strips 1-4 contain 0.1 $\mu$ M target, strips 5-8 contain 0.5 $\mu$ M target. B) Strips 1-4 contain 0.005  $\mu$ M, strips 5-8 contain 0.1  $\mu$ M target. C) Strips 1-4 contain 50pM, strips 5-8 contain 100pM target. 5X SSC was used as RB and negative control for all experiments.

Figure 3.13 results showed that the LOD is detected by 4  $\mu$ M and 8  $\mu$ M probs 2 as 5 nM (strip B1, B3). Thus, this model and optimization is seen as suitable for detection of low concentration of target.



**Figure 3.14 :** Limit of detection experiments using Whatman 1 membrane with Model 1(A-B). A) Strips 1,2,5,6 are 4μM probe, strips 3,4,7,8 are 8μM probe. Strips 1-4 contain 0.1μM, strips 5-8 contain 0.5μM target. B) Strips 1,2,5,6 are 4μM probe, strips 3,4,7,8 are 8μM probe. Strips 1-4 contain a 50pM target, and strips 5-8 contain a 100pM target. 5X SSC was used as RB and negative control for all experiments.

Figure 3.14 results showed that the LOD is detected by 4 μM and 8 μM probes as 0.1 μM (strip A1, A3). Although there is no significant difference between strip A1 and A3, A3 might be used for low detection of SARS-CoV-2 N gene region as the test line intensity is better than A1.



**Figure 3.15 :** Limit of detection experiments using Whatman 1 membrane with Model 2 (A-B). Strips 1,2,5,6 are 4 $\mu$ M, strips 3,4,7,8 are 8 $\mu$ M. A) Strips 1-4 contain 0.1 $\mu$ M target, strips 5-8 contain 5 nM target. B) Strips 1-4 contain 50pM targets, strips 5-8 contain 100pM targets. 5X SSC is used as RB and negative control for all experiments.

Figure 3.15 results showed that the LOD is detected by 4  $\mu$ M and 8  $\mu$ M probes as 5 nM (strip A5, A7). While there is no significant difference between the strip A5 and A7, A7 is seen as the best assay for low detection of SARS-CoV-2 N gene region compared to the all developed strips.

#### 4. CONCLUSION

In this study, LFT strips were developed using colloidal AuNP to detect COVID-19 caused by SARS-CoV-2. This test platform is based on the visual detection of target sequences with the sandwich hybridization model. The main advantage of hybridization is that the target does not need to be labelled. The test was performed on a nitrocellulose membrane having a target specific detection oligonucleotide and target specific probe conjugated on AuNP. Optimization of the test platform was experienced using different running and sample pad buffers, applying temperature values, membranes, sandwich model types and probe concentrations present on AuNPs for the detection of conserved sequence of SARS-CoV-2 N gene region approved by WHO. According to the results, 5X SSC running buffer is suitable because of not having nonspecific binding and Whatman 2 membrane with sandwich model 1 is also the best model for developed LFT for the synthetic target and PCR product. LOD studies demonstrated that 5nM target might be recognized specifically and selectively by developed strip tests.

In summary, the findings showed that the developed LFT, which gives the result in 5-7 minutes, can be used to detect SARS-CoV-2. The real PCR product of N gene region of SARS-CoV-2 was recognized in parallel to the synthetic target gene detection by developed LFT. To the best of our knowledge this study is the first demonstrating that LFTs can be used in the molecular diagnosis of SARS CoV-2 by designing these sandwich models. Designed platform also have potential to be developed for new mutated forms of SARS-CoV-2 since our test principle is based on the molecular recognition of various gene regions. Therefore, the test platform developed in this study can be considered as a fast, accurate, easy-to-use and cost-effective detection method for SARS-CoV-2.

## REFERENCES

- Al-Hazmi, A.** (2016). Challenges presented by MERS corona virus, and SARS corona virus to global health. *Saudi journal of biological sciences*, 23(4), 507-511.
- Araf, Y., Faruqui, N. A., Anwar, S., & Hosen, M. J.** (2020). SARS-CoV-2: a new dimension to our understanding of coronaviruses. *International Microbiology*, 1-6.
- Arya, R., Kumari, S., Pandey, B., Mistry, H., Bihani, S. C., Das, A., ... & Kumar, M.** (2021). Structural insights into SARS-CoV-2 proteins. *Journal of molecular biology*, 433(2), 166725.
- Astuti, I.** (2020). Severe Acute Respiratory Syndrome Coronavirus 2 (SARS-CoV-2): An overview of viral structure and host response. *Diabetes & Metabolic Syndrome: Clinical Research & Reviews*, 14(4), 407-412.
- Broughton, J. P., Deng, X., Yu, G., Fasching, C. L., Servellita, V., Singh, J., ... & Chiu, C. Y.** (2020). CRISPR–Cas12-based detection of SARS-CoV-2. *Nature biotechnology*, 38(7), 870-874.
- Cai, X. F., Chen, J., li Hu, J., Long, Q. X., Deng, H. J., Liu, P., ... & Wang, D. Q.** (2020). A peptide-based magnetic chemiluminescence enzyme immunoassay for serological diagnosis of coronavirus disease 2019. *The Journal of infectious diseases*, 222(2), 189-193.
- Cameron, M. J., Bermejo-Martin, J. F., Danesh, A., Muller, M. P., & Kelvin, D. J.** (2008). Human immunopathogenesis of severe acute respiratory syndrome (SARS). *Virus research*, 133(1), 13-19.
- Chen, N., Zhou, M., Dong, X., Qu, J., Gong, F., Han, Y., ... & Zhang, L.** (2020). Epidemiological and clinical characteristics of 99 cases of 2019 novel coronavirus pneumonia in Wuhan, China: a descriptive study. *The lancet*, 395(10223), 507-513.
- Chu, D. K., Poon, L. L., Gomaa, M. M., Shehata, M. M., Perera, R. A., Zeid, D. A., ... & Kayali, G.** (2014). MERS coronaviruses in dromedary camels, Egypt. *Emerging infectious diseases*, 20(6), 1049.
- Corman, V. M., Landt, O., Kaiser, M., Molenkamp, R., Meijer, A., Chu, D. K., ... & Drosten, C.** (2020). Detection of 2019 novel coronavirus (2019-nCoV) by real-time RT-PCR. *Eurosurveillance*, 25(3), 2000045.
- Cui, J., Li, F., & Shi, Z. L.** (2019). Origin and evolution of pathogenic coronaviruses. *Nature Reviews Microbiology*, 17(3), 181-192..
- De, D., & Pandhi, D.** (2020). Use of immunosuppressants/immunomodulators in autoimmune/inflammatory dermatologic diseases during COVID-19 pandemic —General recommendation based on available evidence. *Indian Dermatology Online Journal*, 11(4), 526.
- De Haan, C. A., De Wit, M., Kuo, L., Montalto-Morrison, C., Haagmans, B. L., Weiss, S. R., ... & Rottier, P. J.** (2003). The glycosylation status of the murine hepatitis coronavirus M protein affects the interferogenic capacity of the virus in vitro and its ability to replicate in the liver but not the brain. *Virology*, 312(2), 395-406.
- De Wit, E., Rasmussen, A. L., Falzarano, D., Bushmaker, T., Feldmann, F., Brining, D. L., ... & Munster, V. J.** (2013). Middle East respiratory syndrome coronavirus (MERS-CoV) causes transient lower respiratory tract infection in rhesus

macaques. *Proceedings of the National Academy of Sciences*, 110(41), 16598-16603.

- Drosten, C., Gunther, S., Preiser, W., van der Werf, S., Brodt, H.-R., Becker, S., Rabenau, H., Panning, M., Kolesnikova, L., Fouchier, R.A.M., Berger, A., Burguiere, A.-M., Cinatl, J., Eickmann, M., Escriou, N., Grywna, K., Kramme, S., Manuguerra, J.-C., Muller, S., Rickerts, V., Sturmer, M., Vieth, S., Klenk, H.-D., Osterhaus, A.D.M.E., Schmitz, H., Doerr, H.W.,** 2003. Identification of a novel coronavirus in patients with severe acute respiratory syndrome. *N. Engl. J. Med.* 348, 1967–1976
- Ejazi, S. A., Ghosh, S., & Ali, N.** (2021). Antibody detection assays for COVID-19 diagnosis: an early overview. *Immunology and Cell Biology*, 99(1), 21-33.
- El-Kafrawy, S. A., El-Daly, M. M., Hassan, A. M., Kaki, R. M., Abuzenadah, A. M., Kamal, M. A., & Azhar, E. I.** (2021, January). A Direct Method for RT-PCR Detection of SARS-CoV-2 in Clinical Samples. In *Healthcare* (Vol. 9, No. 1, p. 37). Multidisciplinary Digital Publishing Institute.
- Fehr, A. R., HJ, P. S. M., Bickerton, E., & Britton, P.** (2015). An Overview of Their Replication and Pathogenesis; Section 2 Genomic Organization. *Methods in Molecular Biology. Springer*, 1282, 1-23.
- Grabar, K. C., Freeman, R. G., Hommer, M. B., & Natan, M. J.** (1995). Preparation and characterization of Au colloid monolayers. *Analytical chemistry*, 67(4), 735-743.
- Graham, R. L., & Baric, R. S.** (2010). Recombination, reservoirs, and the modular spike: mechanisms of coronavirus cross-species transmission. *Journal of virology*, 84(7), 3134-3146.
- Guo, Y., Korteweg, C., McNutt, M. A., & Gu, J.** (2008). Pathogenetic mechanisms of severe acute respiratory syndrome. *Virus research*, 133(1), 4-12.
- Harapan, H., Itoh, N., Yufika, A., Winardi, W., Keam, S., Te, H., Megawati, D., Hayati, Z., Wagner, A.L., Mudatsir, M.** 2020. “Coronavirus disease 2019 (COVID-19): A literature review,” *J. Infect. Public Health*, vol. 13, no. 5, pp. 667–673, doi: 10.1016/j.jiph.2020.03.019.
- Hatcher, E.L., Bao, Y., Blinkova, O., Nawrocki, E.P., Ostapchuck, Y., Zhdanov, S.A.,** ark. 2017. “Virus variation resource dimproved response to emergent viral outbreaks”, *Nucleic Acids Res*, 45(D1):D482-D490. doi: 10.1093/nar/gkw1065.
- Hatmal, M. M. M., Alshaer, W., Al-Hatamleh, M. A., Hatmal, M., Smadi, O., Taha, M. O., ... & Plebanski, M.** (2020). Comprehensive Structural and Molecular Comparison of Spike Proteins of SARS-CoV-2, SARS-CoV and MERS-CoV, and Their Interactions with ACE2. *Cells*, 9(12), 2638.
- Heald-Sargent, T., & Gallagher, T.** (2012). Ready, set, fuse! The coronavirus spike protein and acquisition of fusion competence. *Viruses*, 4(4), 557-580.
- Hoffmann, M., Kleine-Weber, H., Schroeder, S., Krüger, N., Herrler, T., Erichsen, S., ... & Pöhlmann, S.** (2020). SARS-CoV-2 cell entry depends on ACE2 and

TMPRSS2 and is blocked by a clinically proven protease inhibitor. *cell*, 181(2), 271-280.

- Hong, M., Mandala, V., McKay, M., Shcherbakov, A., Dregni, A., & Kolocouris, A.** (2020). Structure and drug binding of the SARS-CoV-2 envelope protein in phospholipid bilayers.
- Jiang, S., Hillyer, C.** (2020). Du LJTi. *Neutralizing antibodies against SARS-CoV-2 and other human coronaviruses*, 41, 355-359.
- Kaya, E., Akata, I., Bakırcı, S., Dereli, D., Küçüküven, E., & Yılmaz, İ.** (2014). İMMÜNOKROMATOGRAFİK KART TESTLERİN ÇALIŞMA PRENSİBİ VE ÜRETİM TEKNİKLERİ. *Duzce Medical Journal*, 16(3).
- Kuru, T. T., & Asrat, D.** (2004). Update on virological, epidemiological and diagnostic aspects of Sars-Corona Virus (SARS-CoV): A newly emerging virus. *The Ethiopian Journal of Health Development*, 18(1).
- Lai, C. C., Shih, T. P., Ko, W. C., Tang, H. J., & Hsueh, P. R.** (2020). Severe acute respiratory syndrome coronavirus 2 (SARS-CoV-2) and coronavirus disease-2019 (COVID-19): The epidemic and the challenges. *International journal of antimicrobial agents*, 55(3), 105924.
- Li, C., & Ren, L.** (2020). Recent progress on the diagnosis of 2019 Novel Coronavirus. *Transboundary and emerging diseases*, 67(4), 1485-1491.
- Li, F.** (2016). Structure, function, and evolution of coronavirus spike proteins. *Annual review of virology*, 3, 237-261.
- Lin, D., Liu, L., Zhang, M., Hu, Y., Yang, Q., Guo, J., ... & Zhang, Z.** (2020). Evaluations of the serological test in the diagnosis of 2019 novel coronavirus (SARS-CoV-2) infections during the COVID-19 outbreak. *European Journal of Clinical Microbiology & Infectious Diseases*, 39(12), 2271-2277.
- Liu, Y., Mao, B., & Liang, S.** (2020). Shanghai Clinical Treatment Experts Group for COVID-19, et al. Association between age and clinical characteristics and outcomes of COVID-19. *Eur Respir J*, 55(5), 2001112.
- Ludwig, S., Zarbock, A.** (2020). Coronaviruses and SARS-CoV-2: a brief overview. *Anesthesia and analgesia*.
- Luk, H. K., Li, X., Fung, J., Lau, S. K., & Woo, P. C.** (2019). Molecular epidemiology, evolution and phylogeny of SARS coronavirus. *Infection, Genetics and Evolution*, 71, 21-30.
- O'Farrell, B.** (2009). Evolution in lateral flow-based immunoassay systems. In *Lateral flow immunoassay* (pp. 1-33). Humana Press.
- Padron-Regalado, E.** (2020). Vaccines for SARS-CoV-2: lessons from other coronavirus strains. *Infectious diseases and therapy*, 9(2), 255-274.
- Parashar, N. C., Poddar, J., Chakrabarti, S., and Parashar, G.**, 2020. "Repurposing of SARS-CoV nucleocapsid protein specific nuclease resistant RNA aptamer for therapeutics against SARS-CoV-2," *Infect. Genet. Evol.*, vol. 85, no. August, p. 104497, doi: 10.1016/j.meegid.2020.104497.
- Parolo, C., de la Escosura-Muñiz, A., & Merkoçi, A.** (2013). Enhanced lateral flow immunoassay using gold nanoparticles loaded with enzymes. *Biosensors and Bioelectronics*, 40(1), 412-416.

- Perlman S, Dandekar AA.** (2005). Immunopathogenesis of coronavirus infections: implications for SARS. *Nat Rev Immunol* 2005;5(12):917–27.
- Rahman, M. S., Islam, M. R., Alam, A. R. U., Islam, I., Hoque, M. N., Akter, S., ... & Hossain, M. A.** (2021). Evolutionary dynamics of SARS-CoV-2 nucleocapsid protein and its consequences. *Journal of medical virology*, 93(4), 2177-2195.
- Ruch, T. R., & Machamer, C. E.** (2012). The coronavirus E protein: assembly and beyond. *Viruses*, 4(3), 363-382.
- Saikatendu KS, Buchmeier MJ, Joseph JS, , Subramanian V, Neuman BW, Stevens RC,** ark. 2007. Ribonucleocapsid formation of severe acute respiratory syndrome coronavirus through molecular action of the N-terminal domain of N protein. *J Virol* 81:3913e21.)
- Sajid, M., Kawde, A. N., & Daud, M.** (2015). Designs, formats and applications of lateral flow assay: A literature review. *Journal of Saudi Chemical Society*, 19(6), 689-705.
- Su, S., Wong, G., Shi, W., Liu, J., Lai, A. C., Zhou, J., ... & Gao, G. F.** (2016). Epidemiology, genetic recombination, and pathogenesis of coronaviruses. *Trends in microbiology*, 24(6), 490-502..
- Stasi, C., Fallani, S., Voller, F., & Silvestri, C.** (2020). Treatment for COVID-19: An overview. *European Journal of Pharmacology*, 173644.
- Tekol, S. D.** (2020). SARS-CoV-2: Virolojisi ve Tanıda Kullanılan Mikrobiyolojik Testler. *Southern Clinics of Istanbul Eurasia*.
- Togay A. and Yilmaz N.,** 2020. “Laboratory Diagnosis of SARS-CoV-2,” *J. Tepecik Educ. Res. Hosp.*, vol. 30, pp. 70–75, 2020, doi: 10.5222/terh.13007
- Ujike, M., & Taguchi, F.** (2015). Incorporation of spike and membrane glycoproteins into coronavirus virions. *Viruses*, 7(4), 1700-1725.
- Wang, M. Y., Zhao, R., Gao, L. J., Gao, X. F., Wang, D. P., & Cao, J. M.** (2020). SARS-CoV-2: structure, biology, and structure-based therapeutics development. *Frontiers in cellular and infection microbiology*, 10.
- Wang, W., Xu, Y., Gao, R., Lu, R., Han, K., Wu, G., & Tan, W.** (2020). Detection of SARS-CoV-2 in different types of clinical specimens. *Jama*, 323(18), 1843-1844.
- Wang, Z., Zhi, D., Zhao, Y., Zhang, H., Wang, X., Ru, Y., & Li, H.** (2014). Lateral flow test strip based on colloidal selenium immunoassay for rapid detection of melamine in milk, milk powder, and animal feed. *International Journal of Nanomedicine*, 9, 1699.
- Xiao, K., Zhai, J., Feng, Y., Zhou, N., Zhang, X., Zou, J. J., ... & Shen, Y.** (2020). Isolation and characterization of 2019-nCoV-like coronavirus from Malayan pangolins. *BioRxiv*.
- Xiong, D., Dai, W., Gong, J., Li, G., Liu, N., Wu, W., ... & Tang, G.** (2020). Rapid detection of SARS-CoV-2 with CRISPR-Cas12a. *PLoS biology*, 18(12), e3000978.
- Xu, J., Zhao, S., Teng, T., Abdalla, A. E., Zhu, W., Xie, L., ... & Guo, X.** (2020). Systematic comparison of two animal-to-human transmitted human coronaviruses: SARS-CoV-2 and SARS-CoV. *Viruses*, 12(2), 244.



- Yu, J., Ouyang, W., Chua, M. L., & Xie, C. (2020).** SARS-CoV-2 transmission in patients with cancer at a tertiary care hospital in Wuhan, China. *JAMA oncology*, 6(7), 1108-1110.
- Yücel, B., & Görmez, A. A. (2019).** SARS-Corona virüsüne genel bakış. *Türkiye Teknoloji ve Uygulamalı Bilimler Dergisi*, 2(1), 32-39.
- Zaki, A. M., Van Boheemen, S., Bestebroer, T. M., Osterhaus, A. D., & Fouchier, R. A. (2012).** Isolation of a novel coronavirus from a man with pneumonia in Saudi Arabia. *New England Journal of Medicine*, 367(19), 1814-1820.
- Zhou, P., Yang, X. L., Wang, X. G., Hu, B., Zhang, L., Zhang, W., & Si, H. (2020). R.; Zhu, Y.; Li, B.; Huang, C. L., Chen H.-D., Chen J., Luo Y., Guo H., Jiang R.-D., Liu M.-Q., Chen Y., Shen X.-R., Wang X., Zheng X.-S., Zhao K., Chen Q.-J., Deng F., Liu L.-L., Yan B., Zhan FX, Wang Y.-Y., Xiao G.-F., Shi Z.-L.** A pneumonia outbreak associated with a new coronavirus of probable bat origin. *Nature*, 579, 270-273.
- Zhang, C., Zheng, W., Huang, X., Bell, E. W., Zhou, X., and Zhang, Y. (2020).** Protein Structure and Sequence Reanalysis of 2019-nCoV Genome Refutes Snakes as Its Intermediate Host and the Unique Similarity between Its Spike Protein Insertions and HIV-1. *J. Proteome Res.* 19, 1351–1360. doi: 10.1021/acs.jproteome.0c00129

## **CURRICULUM VITAE**

**Name- Surname:** Enes GÜLTEKİN

### **EDUCATION STATUS:**

**Primary school:** Mersin Primary school / TRABZON

**High school:** Fatih High school /TRABZON

**University Bachelor:** Atatürk University/ ERZURUM

**Master's Degree:** İnönü University/ MALATYA

**Native Language:** Turkish

**Other Language:** Intermediate English

**Computer skills:** Word, Exel, Paint